3-27-2007

Evaluation of Unknown Foundations

Ronald W. Florkowski
University of South Florida

Evaluation of Unknown Foundations

by

Ronald W. Florkowski

A thesis submitted in partial fulfillment
of the requirements for the degree of
Master of Science in Civil Engineering
Department of Civil & Environmental Engineering
College of Engineering
University of South Florida

Major Professor: Gray Mullins, Ph.D., P.E.
Rajan Sen, Ph.D., P.E.
Abla Zayed, Ph.D.

Date of Approval:
March 27, 2007

Keywords: sonic echo / impulse response, scour critical, erosion, non-destructive testing, bridge inspections

Table of Contents

List of Figures

Evaluation of Unknown Foundations

Ronald W. Florkowski

ABSTRACT

In recent years, bridge foundations have been in the spotlight throughout the nation. Bridges built over running water are susceptible to erosion or scour around their foundations. The reduction in load capacity to piers and abutments pose a safety risk to highway motorists. It has become necessary for engineers to examine and monitor these "scour critical" bridges. The difficulty arises with subsurface foundations of which very little is known about their construction. Hence, the methods applied to analyzing "Unknown Foundations" have become a necessary topic of research.

This thesis explores a method to determine foundation lengths. Similar to Sonic Echo / Impulse Response, this procedure measures reflected shock waves sent through concrete pilings. The technique is non-destructive in nature and is performed near the surface of the foundation. The test is performed on the side of the exposed piling. Current methods are limited by the fact that the tops of most pilings are inaccessible due to pile caps or beams. Often times, pilings are embedded in stiff soils, which have a dampening effect on the stress waves. This thesis employs a method of analysis that will overcome such limitations and provide engineers with another tool to determine subsurface foundation lengths.

Chapter 1 Introduction

1.1 Introduction

There are a number of risks associated with highway travel. Throughout the United States, there have been reports of foundation failures ranging from sinking half a foot to causing total structural collapse of roadways. Figure 1.1 shows one such bridge in New York where an entire bridge span was lost resulting in 10 fatalities. The Federal Highway Administration and state DOT's have recognized the need to examine our current roadways and correct deficiencies that have the potential to be very harmful.

Figure 1.1: I-90 over Schoharie Creek (Courtesy of Northwestern University Infrastructure Technology Institute [6])

Further, as more is learned in the area of extreme event loading scenarios, re-evaluating existing bridge foundation elements has become a paramount concern.

This thesis looks at bridge surveys, with a focus on assessing the capacity of subsurface foundations. It is known that pilings lose strength as the soil around them erodes away. A problem arises when trying to calculate capacities on pilings, of which, very little is known. The challenge is to develop an economical method to evaluate and characterize the length and condition of existing bridge piles below the surface.

One such method is Sonic Echo / Impulse Response (SE/IR). This procedure had evolved as a means to test the integrity and determine length of drilled shafts and driven piles. It is based on the principle that stress waves created by an impact will travel through a foundation and reflect back to the surface when there is a change in stiffness, cross-section or density. As this is a Non-Destructive Test (NDT) it does not require coring or drilling through bridge components. The test is conducted at the ground surface or top of foundation element. However, there are limitations to the SE/IR method.

One limitation is that testing performed through an existing pile cap or beam is difficult. The large cross-section and interface with the pile or shaft creates reflections that are difficult to interpret. For this case, columnar shaped piles or shafts need to be exposed above the ground or water where testing can be performed on the side. Studies have shown that pilings embedded in stiff soils tend to absorb wave energy, therefore preventing identifiable reflections. In theory, a larger impact delivered to a side-mounted bracket will provide the energy necessary to perform the test. Should, at some point, the required energy approach the driving energy (e.g. pile driving hammer), then it would not be reasonable for existing structures.

1.2 Project Objective

The goal of this thesis is to introduce several improvised methods of examining stress wave propagation delivered to concrete piles for determining unknown foundation lengths. Typically, impact forces originate from the top of piles. A comparison is made to waveforms developed by lateral impacts to the side and then to a mounted bracket on the pile to produce axial impacts at various locations along the length of the pile. The generated waves are measured by a set of accelerometers. Sets of strain gages have also been utilized to augment data collection and waveform analysis.

1.3 Organization of Thesis

This report is organized into four subsequent chapters. Chapter 2 begins with the history of "Unknown Foundations" and then gives an overview of current testing methods in use today. Chapter 3 describes the equipment used for this project and explains the procedure for data collection. Chapter 4 discusses stress wave propagation and includes the concept of frequency analysis. Finally, chapter 5 summarizes the results of trial studies.

Chapter 2 Background

2.1 History of Unknown Foundations

Out of a half million bridges nationwide, over 100,000 have unknown foundations. More than 20,000 of these are considered “scour critical” and susceptible to collapse. Years and years of erosion have taken a toll. The loss of foundation embedment has resulted in reduced loading capacities; some more serious than others. The problem is, deciding which roadway is worse. Many older bridges lack information on design or actual as-built construction records. Without knowledge of foundation dimension, material, depth or condition, a proper assessment cannot be made. Engineers must rely on subsurface testing to characterize structural elements below ground.

2.2 Current Testing Methods

A number of methods have been developed to investigate the unknown foundation depth below ground. Applications vary depending on the type of foundation; that is, timber, steel or masonry. Labor and cost are also important factors.

Ground excavation, although very reliable, is probably the most expensive and least practical method. The process requires heavy equipment, dewatering, closing roadways and is generally dangerous work.

Probing with a rod and hammer is less dangerous, but also physically demanding. It may be helpful with shallow elements, but still leaves a lot of uncertainty. For example, hammering a rod into bedrock could easily be confused for a solid foundation element.

The method of coring may be applied to exposed foundations. Drilling into the element creates the need to repair damage. Similar to rod & hammer, it is used for shallow elements. It is not useful in determining pile depths.

The borehole radar method may be used to determine pile geometry and depth. The technique involves installing a PVC-encased borehole in close proximity of the foundation. Radar energy is transmitted into the surrounding soil. A receiver records reflection produced at interfaces of material with different dielectric properties (Figure 2.1). The reflection of electromagnetic wave energy off steel is strong, which makes it particularly useful in identifying reinforced concrete pilings.

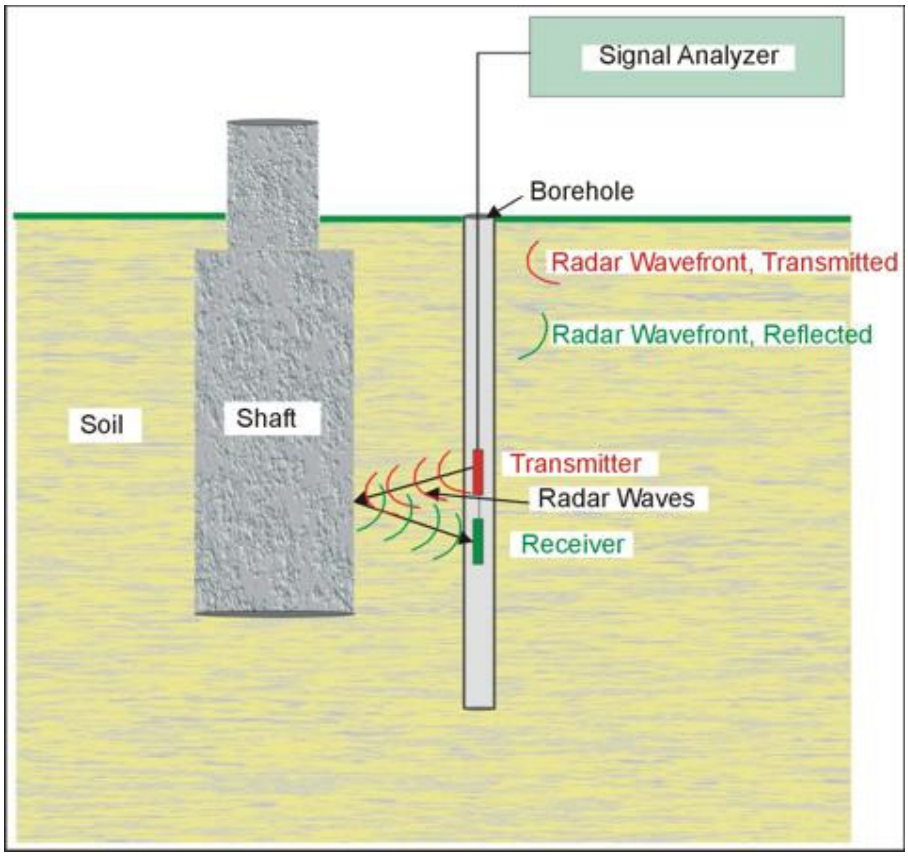

Figure 2.1: Borehole Radar Method (Courtesy of FHWA – Geophysical Imaging Resource Website [3])

Cross Borehole Seismic Tomography is a similar technique that incorporates multiple boreholes through which signals may be transmitted (Figure 2.2). By varying the depth of transmitter and receiver, a two or three dimensional velocity image may be produced (Figure 2.3).

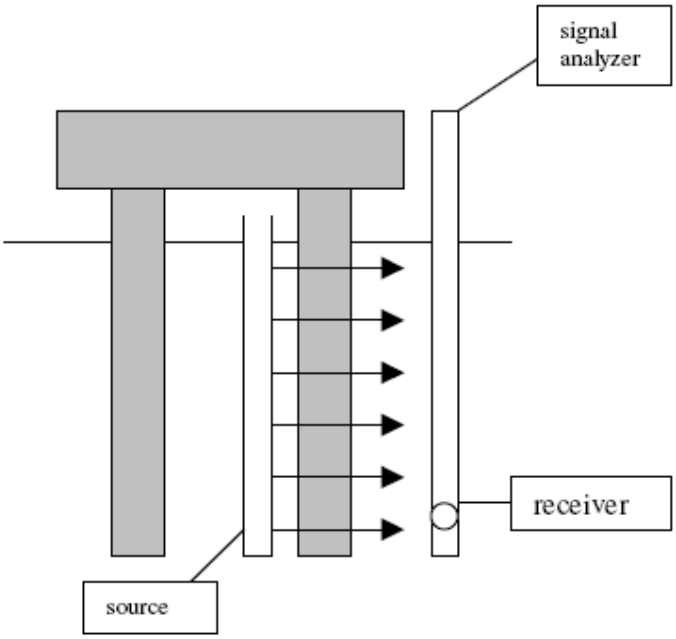

Figure 2.2: Cross Borehole Seismic Tomography

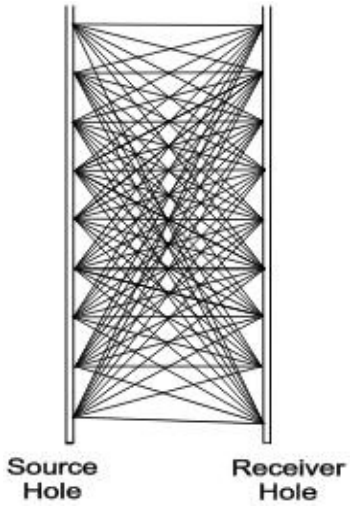

Figure 2.3: Mapping Between Boreholes (Courtesy of FHWA – Geophysical Imaging Resource Website [3])

Both methods have limited use in certain environments, such as conductive clays or salt-water saturated soils where signal interference would be expected. Another disadvantage is that it requires installation of one or more access casings, which is associated with higher time and cost.

Parallel seismic is a method that also requires a borehole in close proximity to the foundation (Figure 2.4). An impact is delivered to exposed structural elements creating seismic wave energy that travels down below the surface.

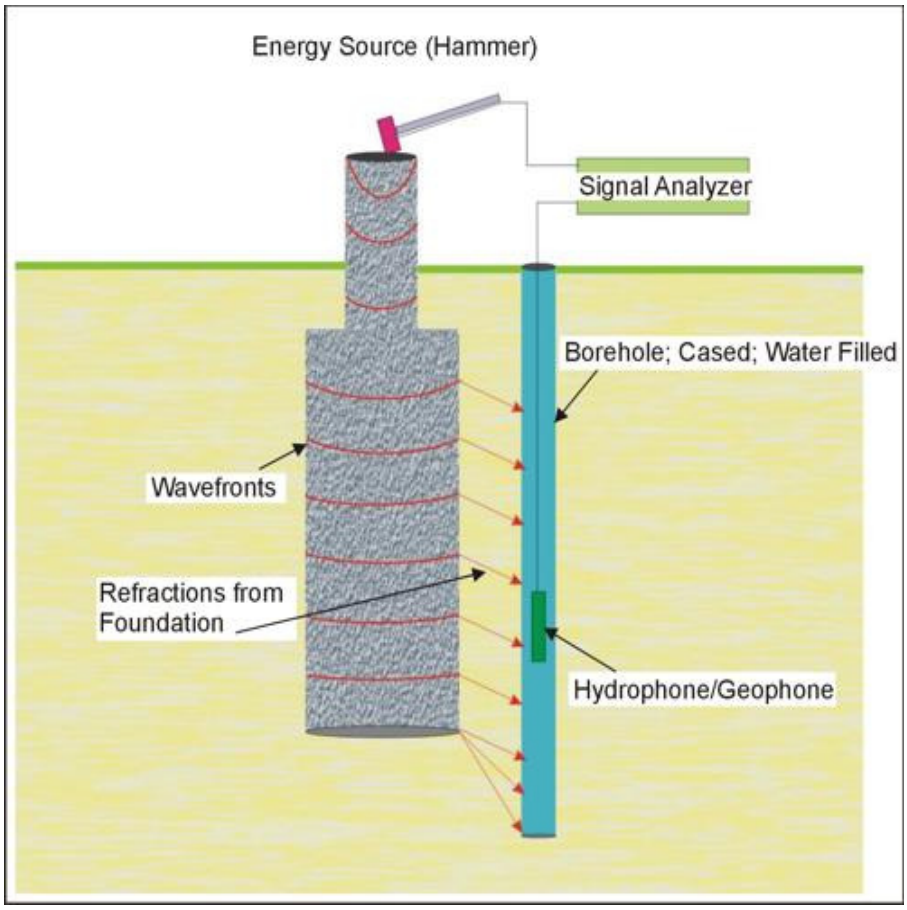

Figure 2.4: Parallel Seismic Method (Courtesy of FHWA – Geophysical Imaging Resource Website [3])

Receivers in the adjacent borehole track changes in wave energy along the piling or shaft. When the receiver is lowered below the toe, the signal weakens. This indicates the depth of foundation. Figure 2.5 is an example of parallel seismic data.

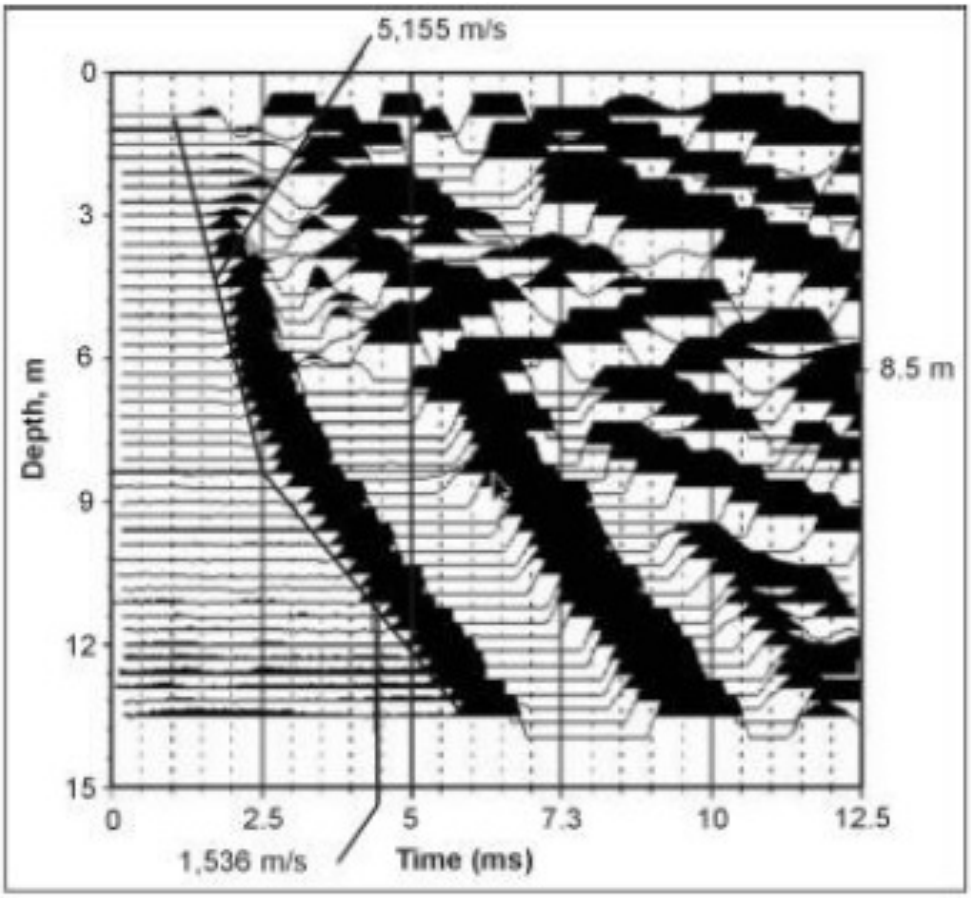

Figure 2.5: Parallel Seismic Data (Courtesy of FHWA – Geophysical Imaging Resource Website [3])

The induction field method also requires a PVC-encased borehole through which a sensor is lowered (Figure 2.6). An oscillating electric current is sent through the conductive material of a foundation, such as reinforcing rebar, to produce a magnetic field. As the sensor is lowered below a foundation, the magnetic field strength drops. This indicates the foundation depth.

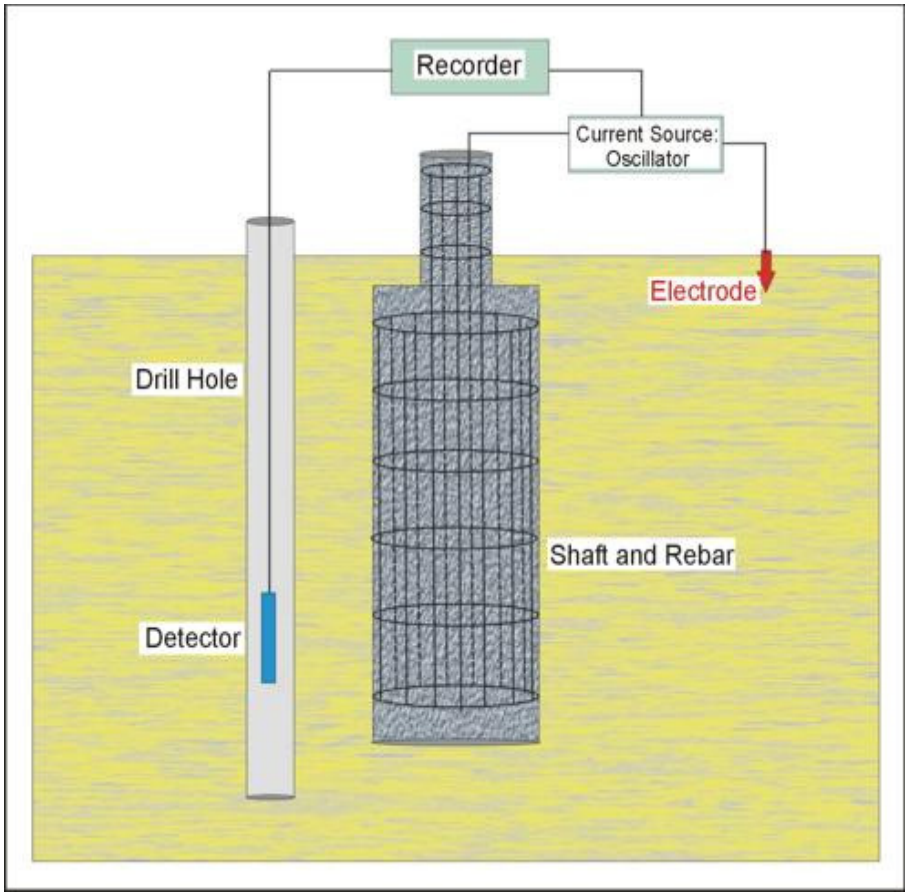

Figure 2.6: Induction Field Method (Courtesy of FHWA – Geophysical Imaging Resource Website [3])

The most important requirement with this method is electrical conductivity. Metal within a pile or shaft must extend the full length and be accessible from the surface. There are limitations in certain environments. Conductive materials in bridge components or soils may interfere with signals.

Sonic echo/impulse response measures the reflection of stress waves created by an impact to an element. It would appear to be the most economical means to determine pile depth. The testing procedure is far less invasive then the aforementioned methods. Figure 2.7 shows a typical application of the test. Two positions on top of the shaft are cleaned and prepped. Tapping the surface occurs at the center. An accelerometer is

secured to the second position, which is off-center, but within the perimeter of the reinforcement cage. A laptop is commonly used to acquire data and process signals.

Figure 2.7: Sonic/Echo Impulse Testing Equipment (Courtesy of Mullins G., et al, "Thermal Integrity Testing of Drilled Shafts," [5])

When a hammer strikes the structure, it causes a distortion and sends a compressive wave down the shaft. The time it takes for the stress wave to reflect off the toe and return to the surface is a function of wave velocity and length of the shaft. Any alteration is due to a change in impedance, such as a change in cross-section, material density or possibly damage to the shaft. Mechanical impedance, Z, is a measure of how much a structure resists motion when subjected to a given force. The impedance is a ratio of the force, F, to the velocity, v, at a point and is a function of frequency, ω:

$$F(\omega) = Z(\omega)v(\omega)$$

Part of the stress wave is reflected back to the surface when there is a change in impedance, while the remaining wave continues to the toe and back. Figure 2.8 is an example output showing the initial impact and return wave from which a shaft length can be calculated. Signal changes in between indicate a change in impedance. There is generally a response limit for stress wave reflection based on a length / diameter ratio and characteristics of the soil. Stiff soils will absorb all energy traveling down shafts with L / D ratios greater than 30:1. Soft soils will allow energy travel in shafts with L / D ratio as high as 50:1.

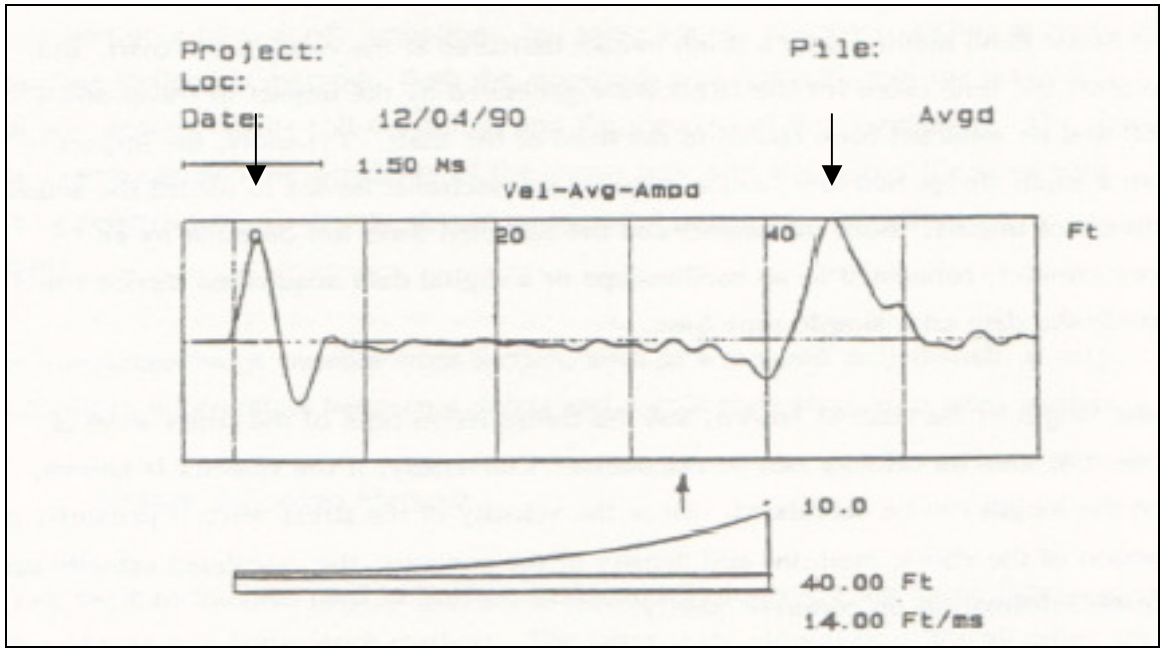

Figure 2.8: Sonic/Echo Impulse Test Results (Courtesy of Mullins G., et al, "Thermal Integrity Testing of Drilled Shafts," [5])

Chapter 3 Methods to Obtain Data

3.1 Introduction

Although sonic/echo impulse testing has proven reliable in certain circumstances, methods to remove inherent limitations for unknown foundation applications could prove fruitful. Figure 2.6 shows a typical application of the sonic/echo impulse test. This thesis introduces a similar application, but with the addition of multiple accelerometers and/or strain gages. The study looks at axial impacts delivered from the side of pilings and lateral impacts as well as the traditional top-of-pile impact. Tapping the surface of a specimen produces compression waves that produce characteristic reflections that are typically recorded by accelerometers, but in this case wave direction, speed and foundation length can also be determined. Two test programs were conducted; (1) lab scale, where equipment and methods were explored and (2) field scale, where full-length piles were tested.

3.2 Equipment and Procedure

3.2.1 Lab Scale Trials

Experiments were conducted in the lab to study the effectiveness of utilizing strain gages in addition to accelerometers to record compression waves. Impacts were delivered to the lateral face of the pile, a mounted steel bracket and the top surface. Figure 3.1 shows the 9-foot, concrete pre-stressed piling positioned vertically in the lab.

Two steel brackets were attached to the 6” x 6” piling. One was bolted at the top. The second was secured midway; a distance 4 feet from the top.

Figure 3.1: Concrete Piling in Lab 6”x 6”x 9’

Four PL-60-11 strain gauges were mounted equally spaced 2 feet apart and centered on the same face of the piling. They were sequentially numbered beginning with number 1 mounted 1 foot from the top. A bonding adhesive was used to secure the gages directly centerline on the piling (Figure 3.2). The PL series gage is a standard 120 Ω wire strain gage with a transparent backing impregnated with a polyester resin. The wire is a Cu-Ni alloy and has an operating temperature range of –20 to 80°C. The gage is 60mm x

1 mm in size and the polyester backing is 74mm x 8mm. The size and durability of the gage makes it easy to apply.

Figure 3.2: Strain Gage PL-60-11

Two accelerometers were utilized; each with a distinct fundamental principle of operation. A piezoelectric accelerometer consists of a quartz crystal. A mass within the component and applied accelerations create forces that deflect the lattice of the crystal. Displaced electrical charge accumulates on an electrode. The signal is conditioned then analyzed.

A capacitive accelerometer senses a change in electrical capacitance. A diaphragm within the component flexes in response to accelerations. This alters the distance between parallel plates. The resulting change in capacitance varies the output of an energized circuit.

Figure 3.3: Piezoelectric Accelerometer SN45519

Figure 3.4: Capacitive Accelerometer

The accelerometers were secured to a clean surface of the steel bracket with a wax medium. The piezoelectric accelerometer was attached to the top bracket (Figure 3.3). The capacitive accelerometer was secured to the bracket midway (Figure 3.4).

The advantages of each type were reviewed. In general, capacitive devices are more sensitive. Piezoelectric devices tend to be more robust, yet less sensitive. In this application, both types were considered due to uncertainty in the amount of signal that might be generated.

A moderate strike with a 12-ounce hammer was used to create compression waves in the piling.

Data collected showed that instrumentation and data acquisition systems selected, worked sufficiently for field data application (See Appendix A).

3.2.2 Field Scale Testing

Studies in the field were conducted in similar fashion. Figure 3.5 shows a 40-foot, concrete pre-stressed piling positioned horizontally. Two steel brackets were attached to the 12” x 12” piling. One was bolted 3.5” from the top. The second was secured at a point, 7 feet from the top.

Four PL-60 strain gauges were mounted symmetrically spaced 2 feet apart with a 3’ spread, midway, between the second and third gage (Figure 3.6). They were sequentially numbered beginning with number 1 mounted 2 feet from the top.

Two accelerometers were utilized. A piezoelectric accelerometer was mounted on the top bracket (Figure 3.7) and a capacitive accelerometer to the bracket midway (Figure 3.8). Both were found to give reasonable information from the trial study.

A 12-ounce hammer striking the top, lateral side and mounted bracket of the piling generated compression waves.

Figure 3.5: Pre-stressed Concrete Piling 12”x 12”x 40’

Figure 3.6: Strain Gage Positions 12”x 12”x 40’ Piling

Figure 3.7: Piezoelectric Accelerometer SN45519 Mounted to Bracket

Figure 3.8: Capacitive Accelerometer Mounted to Bracket

Chapter 4 Data Analysis & Results

4.1 Stress Wave Propagation

Upon impact to a solid, stress waves are generated which radiate in all directions. Generally, there are three types of waves. Compression waves propagate in the direction of the impact or distortion. Shear waves travel perpendicular to the direction of propagation and will only be present in materials that have a shear stiffness. The third type are called Rayleigh surface waves. These waves propagate over the surface of the solid.

The velocity of stress wave propagation is a function of the material properties. It depends on the elastic modulus, E, Poisson's ratio, υ, and the density, ρ. The compressive wave velocity is given by the equation:

$$v_p = \sqrt{[\, E(1-\upsilon)/\rho(1+\upsilon)(1-2\upsilon)]}$$

Shear wave velocity is a function of the shear modulus, G, and material density. The shear modulus is given by the equation:

$$G = E/2(1-\upsilon)$$

Shear wave propagation is given by the equation:

$$v_s = \sqrt{\,[G/\rho]}$$

Typical compression wave velocities in concrete range from 11484 ft/s to 14765 ft/s, depending on composition, condition and age. Shear wave velocity is generally slightly more than half the compression wave velocity. For concrete, a typical shear wave velocity is 0.61 to 0.54 times the compression wave velocity.

$$v_s = v_p \times \sqrt{[\ (1+\upsilon)(1-2\upsilon)/2(1-\upsilon)^2]}$$

Rayleigh surface waves range from $0.862v_s$ to $0.955v_s$ relative to poisson's ratio of 0 to 0.5. When a compression wave is generated by an impact, it travels down the structure until is meets a change in impedance. This may be a change in composition, cross-sectional area, or a break. The wave is then reflected back to its origin where it can be recorded.

4.2 Frequency Analysis

Data collected from a sonic/echo impulse test is very complex. Waveforms represent multiple sinusoids from many frequencies (Figure 4.1). Common practice in signal processing is to convert data from a time domain to a frequency domain for filtering. In the time domain, amplitude is valued at each time interval. In the frequency domain, the output represents the amount each particular frequency or sinusoid is present in the whole signal. The mathematical formula to convert data to the frequency domain is called The Fast Fourier Transform (FFT). Data represented in Figure 4.1 is converted by a FFT to the frequency domain in Figure 4.2. In this form, it is easier to identify particular frequencies. Unwanted interference or noise can be filtered out. Finally, the signal is converted back to the time domain by an inverse FFT (Figure 4.3).

4.3 Results & Conclusions

The field study performed on a 40' pre-stressed concrete piling was successful. All instrumentation responded well as shown in Figure 4.4. Initial observations, without filtering, show the accelerometers in complete disarray, but there appears to be a wave pattern in the strain gages. Filtering data was based on trial and error. Figure 4.5 shows filtered data in the first strain gage. Care must be taken not to cut out too much. As shown, 2500 hertz appears ideal. Filtering at smaller frequencies, like 500 hertz, results in waveforms that are heavily altered and difficult to interpret.

Figure 4.6 shows filtered strain gage response to a top impact. The sequence of strain gage response clearly shows departure and return of a stress wave. The distance between gage 1 and 4 is 7 feet. With a time of 0.000565682 seconds between peaks, the calculated stress wave velocity is 12,374 feet/second. The time between compression peaks for strain gage 1 is 0.006191042 seconds, which works out to a distance of 76.6 feet. The margin of error is 4.25%. It is an advantage to have multiple gages to calculate or verify standard stress wave velocities. But, it is difficult to be accurate with such a short distance between gages and very short time frame without first filtering.

Figure 4.7 shows filtered strain gage response to a center impact. The pile is experiencing flexural stresses instead of an axial direction. Waveforms are present, but not as distinct. As expected, gages 2 and 3 react simultaneously; as do gages 1 and 4. The slight offset between peaks indicates a slight off-center impact. A pre-trigger time of 0.001 seconds captured the response of gage 1 and 4, but cut off the initial strains of gage 2 and 3. With a calculated shear wave velocity of 3500 to 4000 feet/second, a 0.001 sec. pre-trigger would suffice. The delay was due to the accelerometer set for pre-trigger on a

positive direction. It should have triggered in either case, positive or negative; something to be cognizant of in future tests. It is difficult to see reflections from the toe, but it appears to be between 0.009 and 0.010 seconds. There appears to be a lot of overlap of multiple waves.

Figure 4.8 shows filtered strain gage response to a bracket impact. The complete lack of response is due to the position of the bracket. The impact was on the adjacent face of the pile, 90° from the position of strain gages. This coincides with the neutral axis of the pile.

Accelerometer data was difficult to analyze. Even after filtering out higher frequencies, a stress wave could not be identified. The accelerometers were secured to the steel brackets, which may have created an excess of unwanted vibrations. Since the piling was horizontal, contact with the ground may have interfered with axial wave travel.

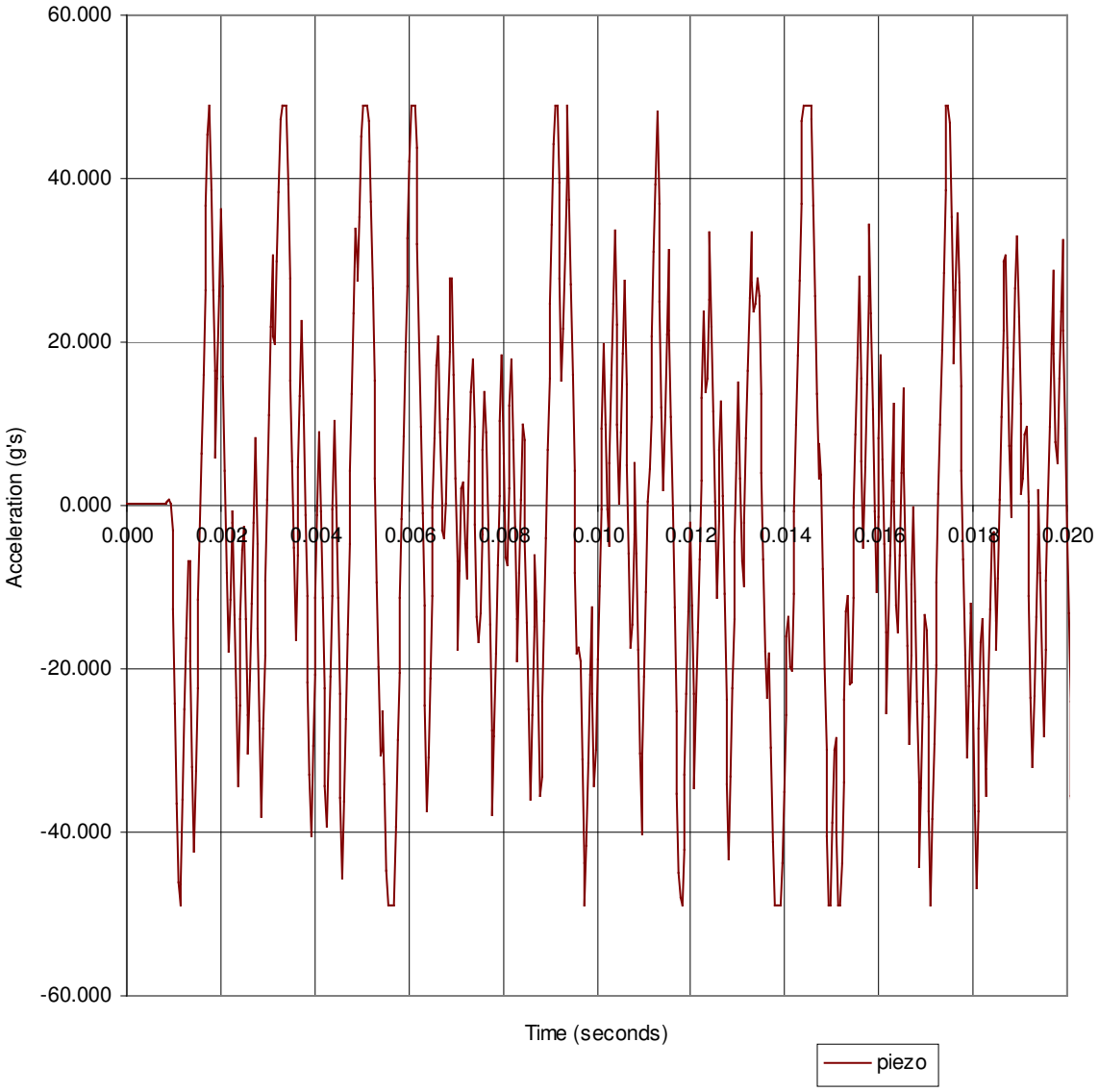

Figure 4.1: Piezoelectric Accelerometer Unfiltered in Time Domain

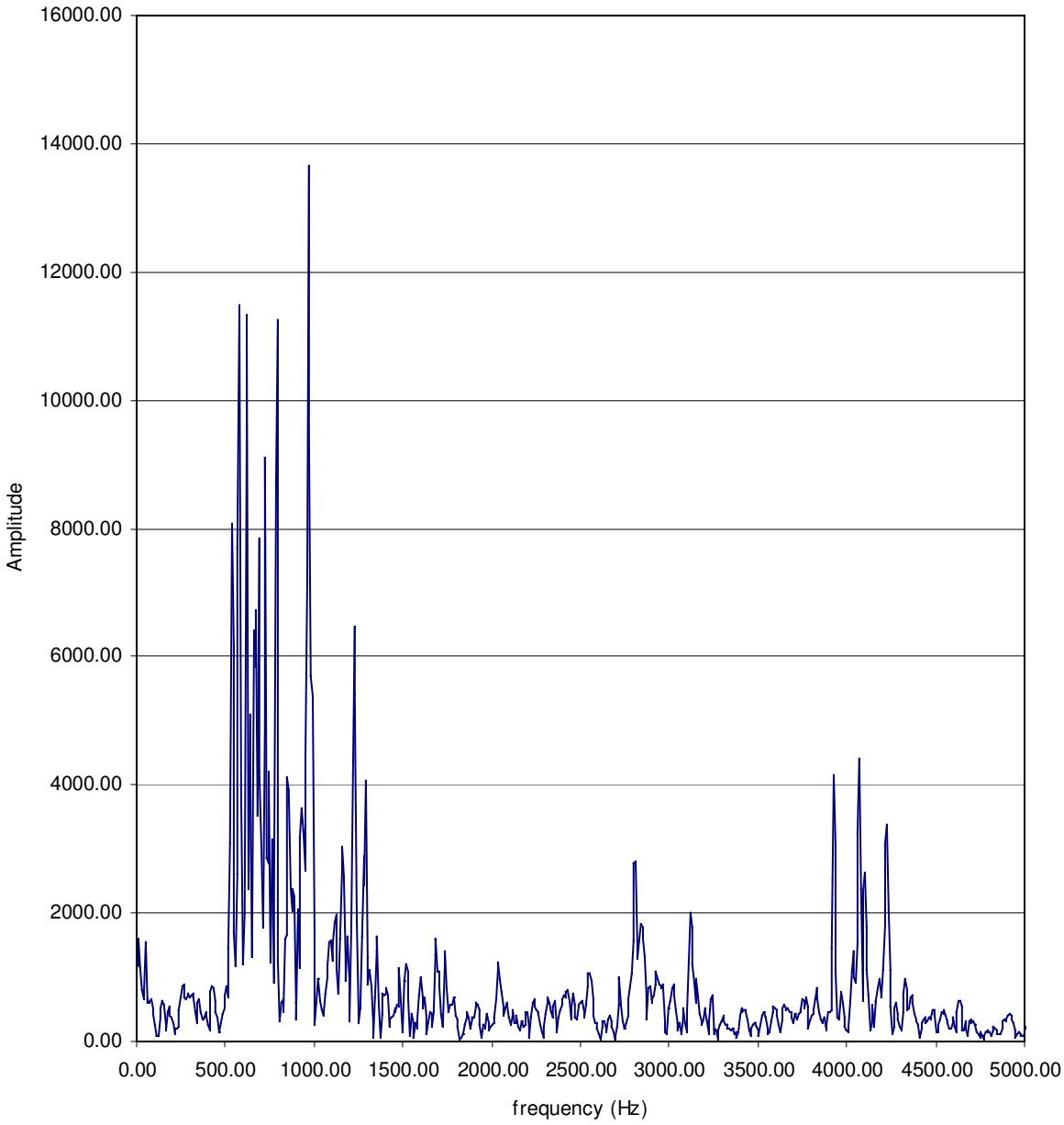

Figure 4.2: Piezoelectric Accelerometer in Frequency Domain

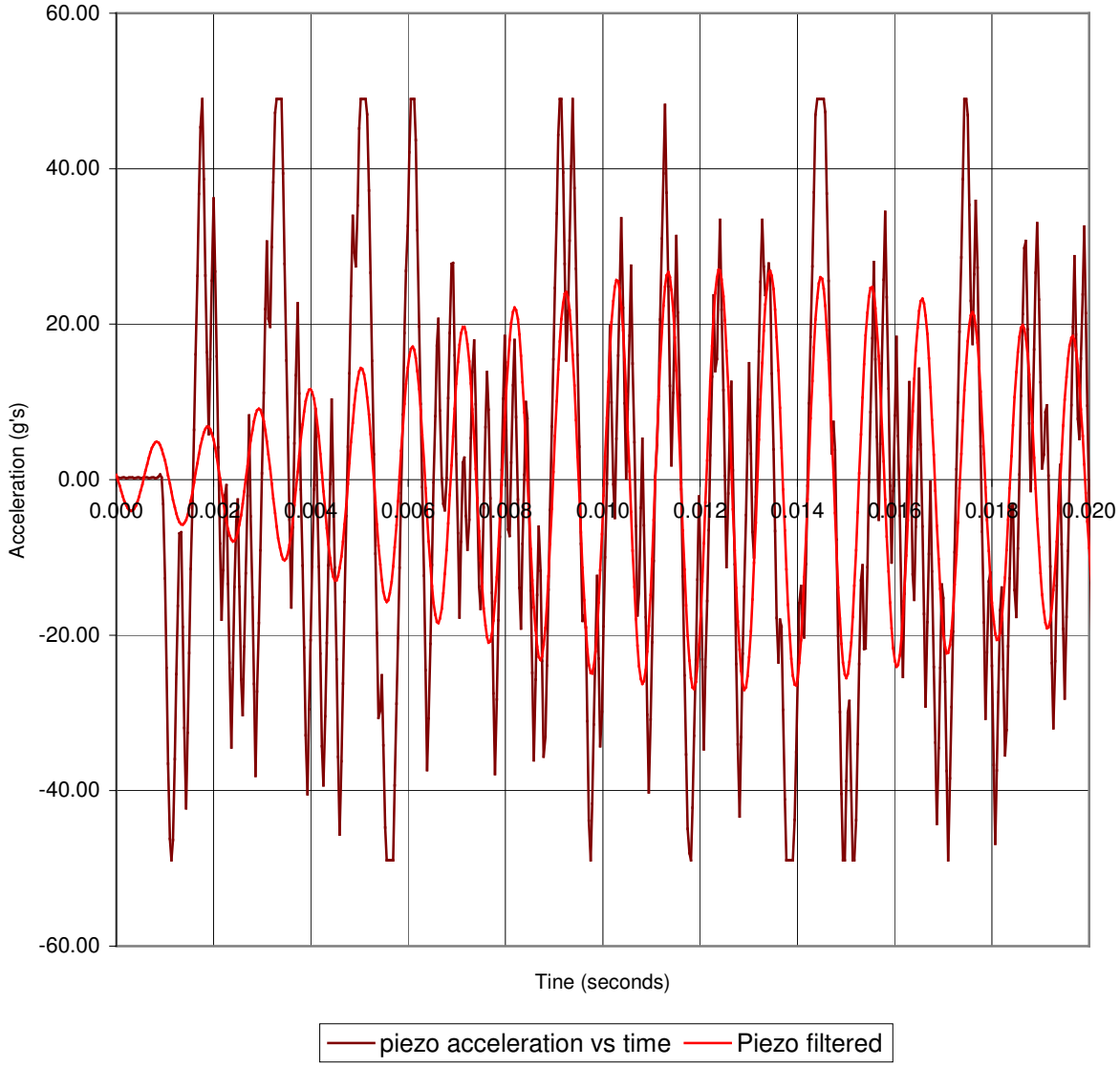

Figure 4.3: Piezoelectric Acceleration Filtered to 1000 Hz

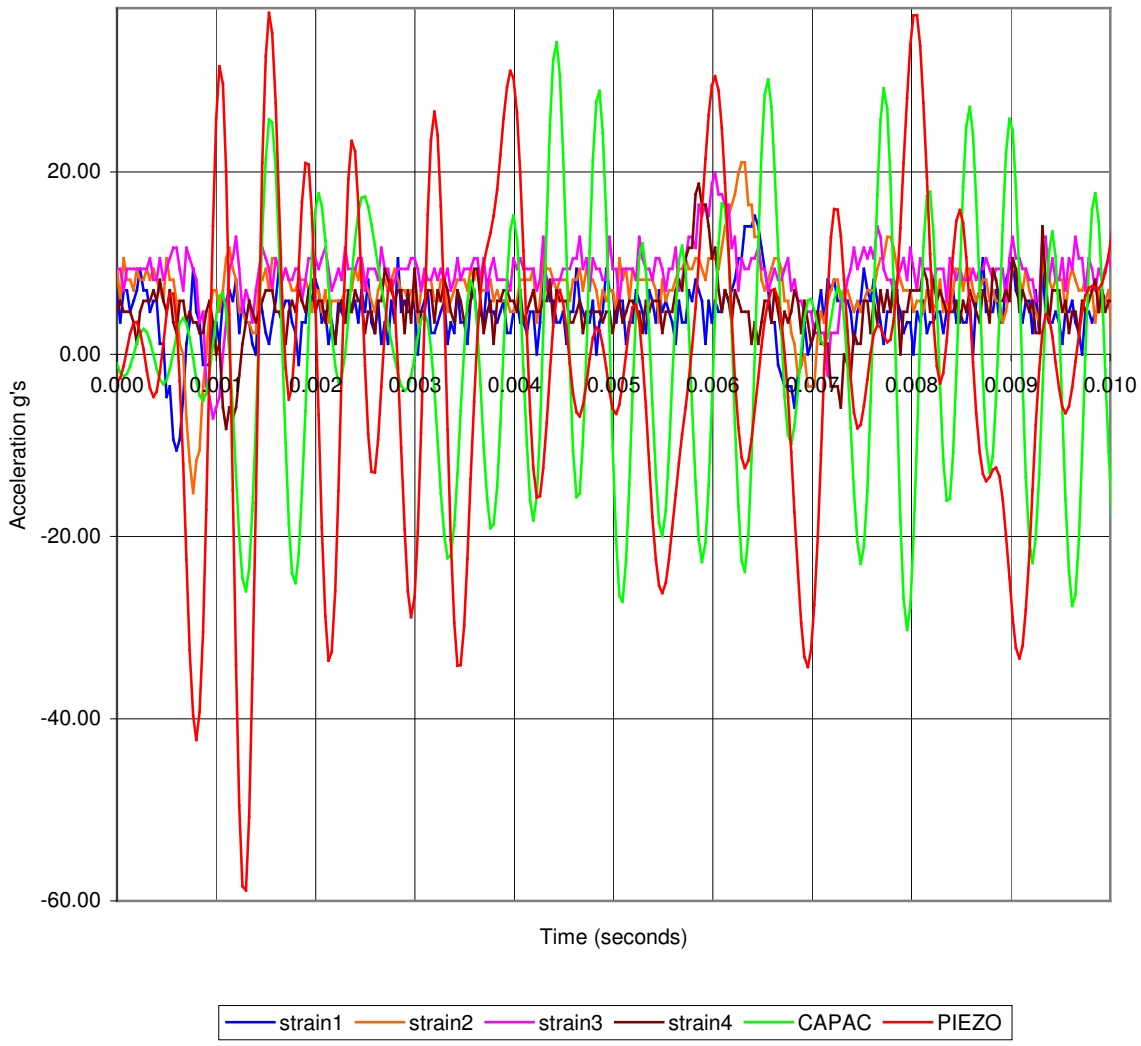

Figure 4.4: Top Impact Strain & Accelerometer Data

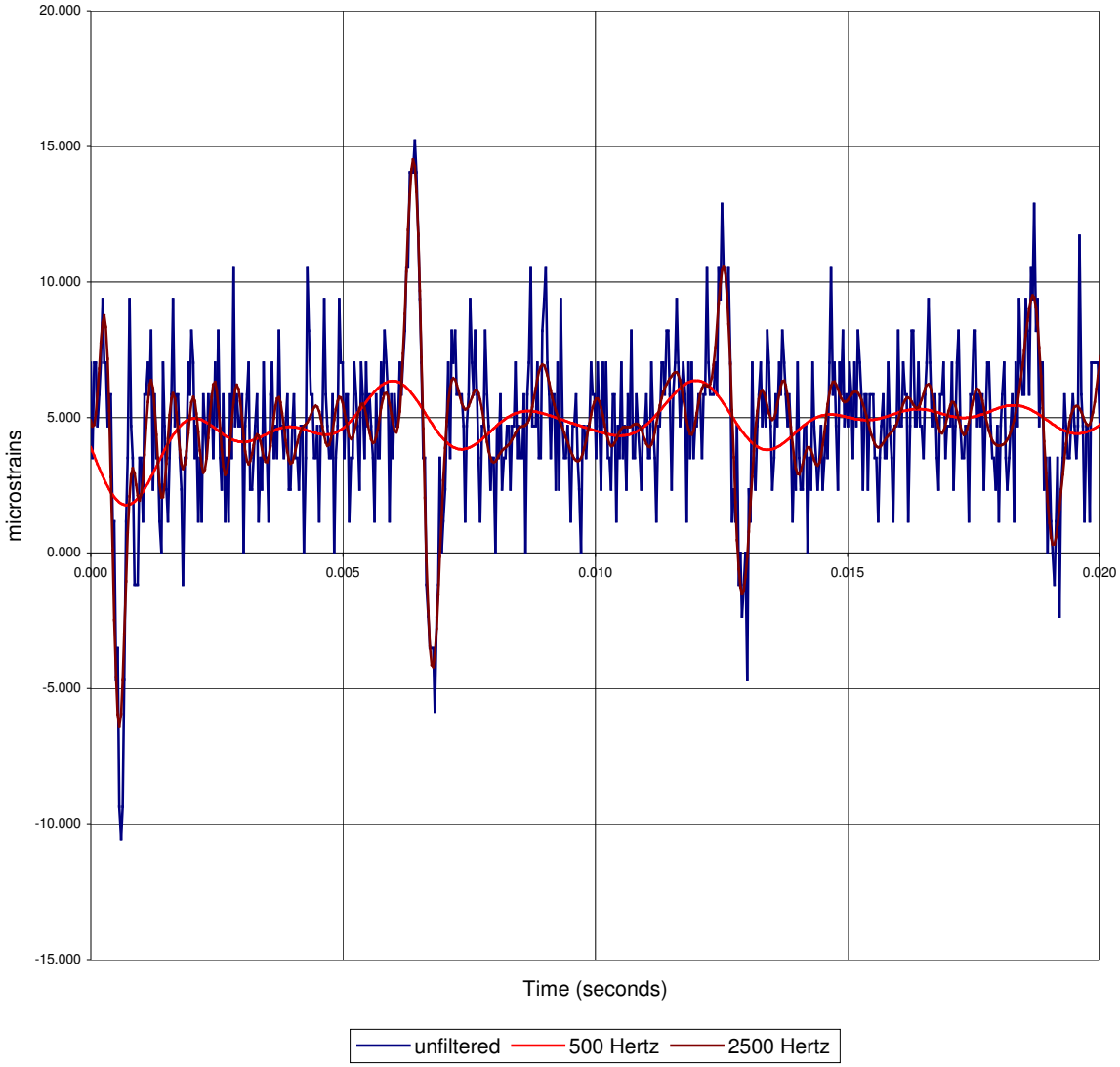

Figure 4.5: Top Impact - Strain 1 Filtered to 2500 Hz

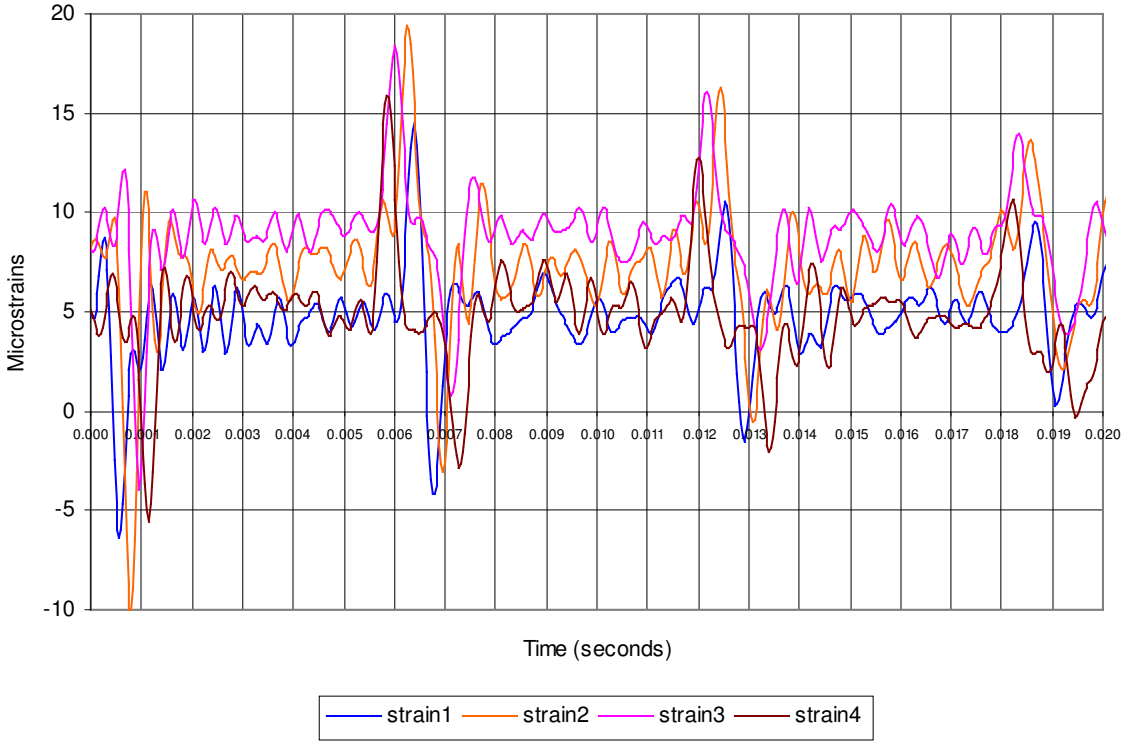

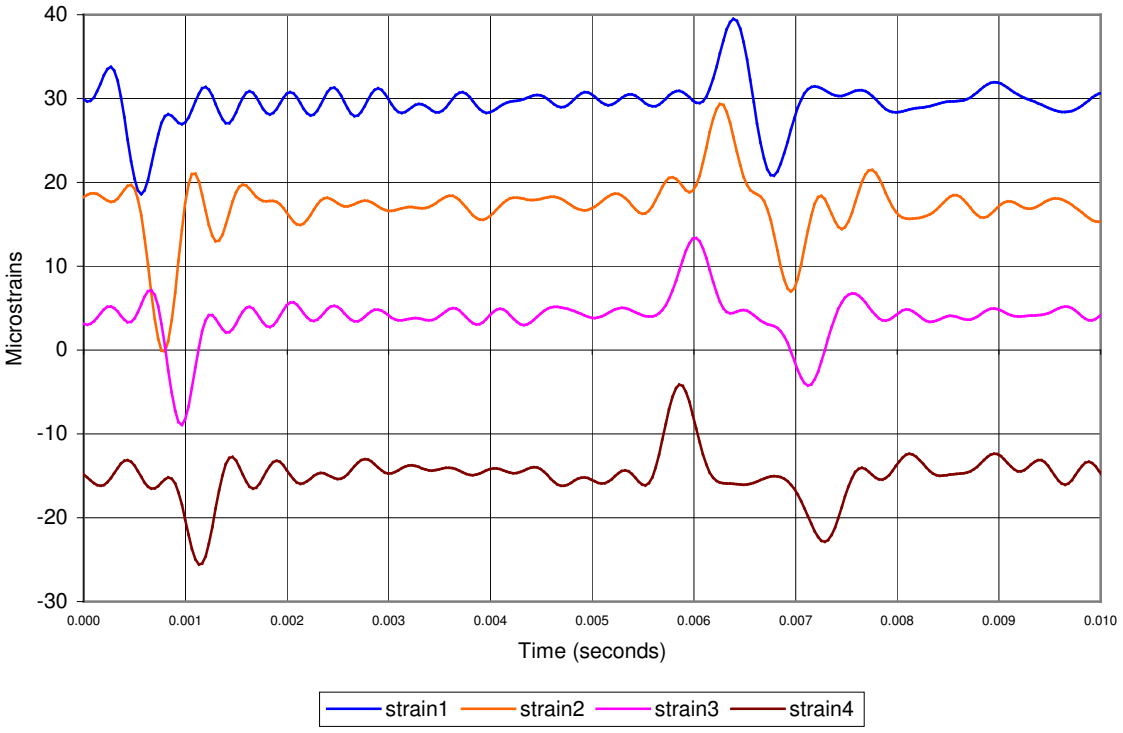

Figure 4.6: Top Impact Strain Gages Filtered to 2500Hz

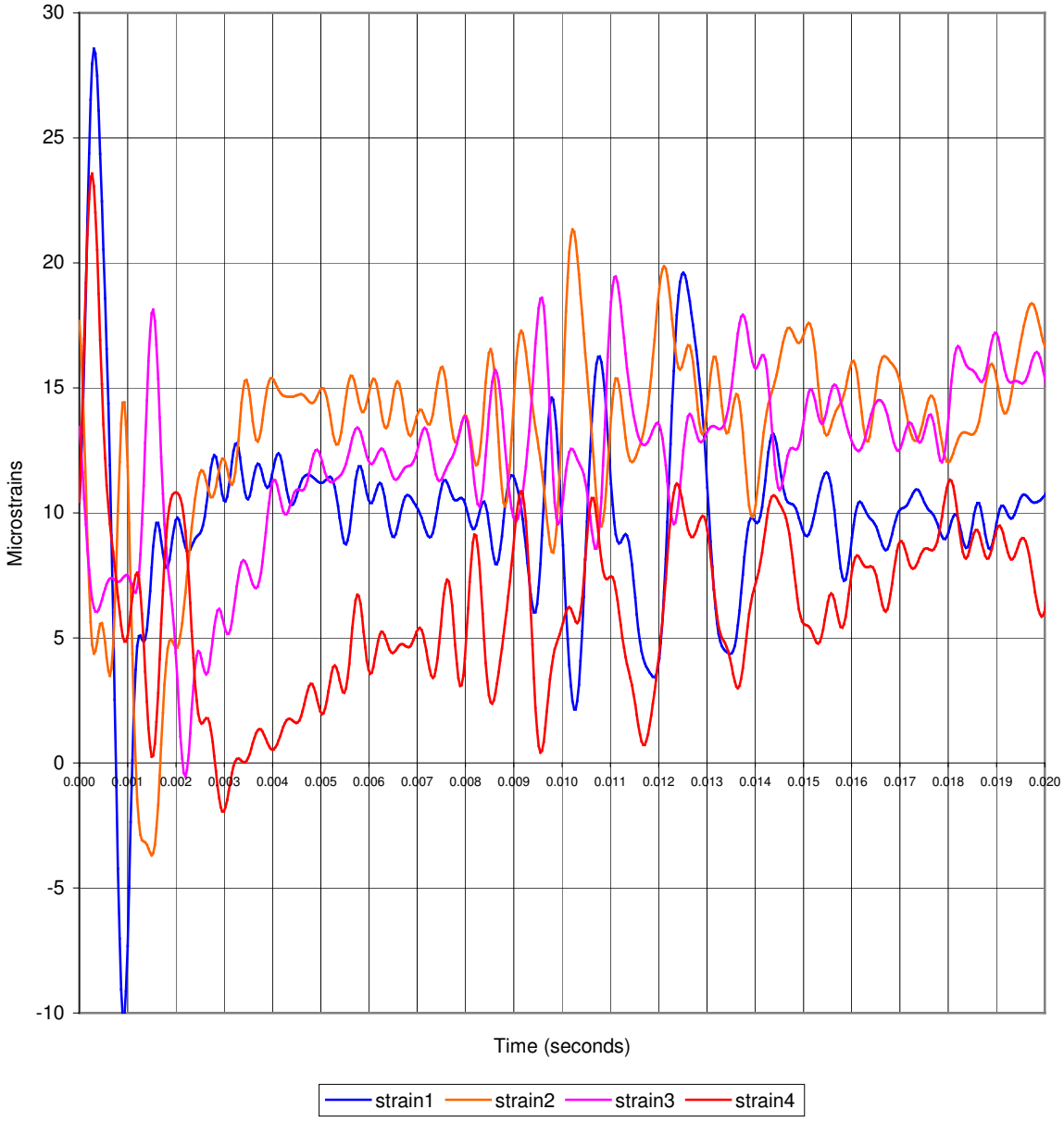

Figure 4.7: Center Impact Strain Gages Filtered to 2500Hz

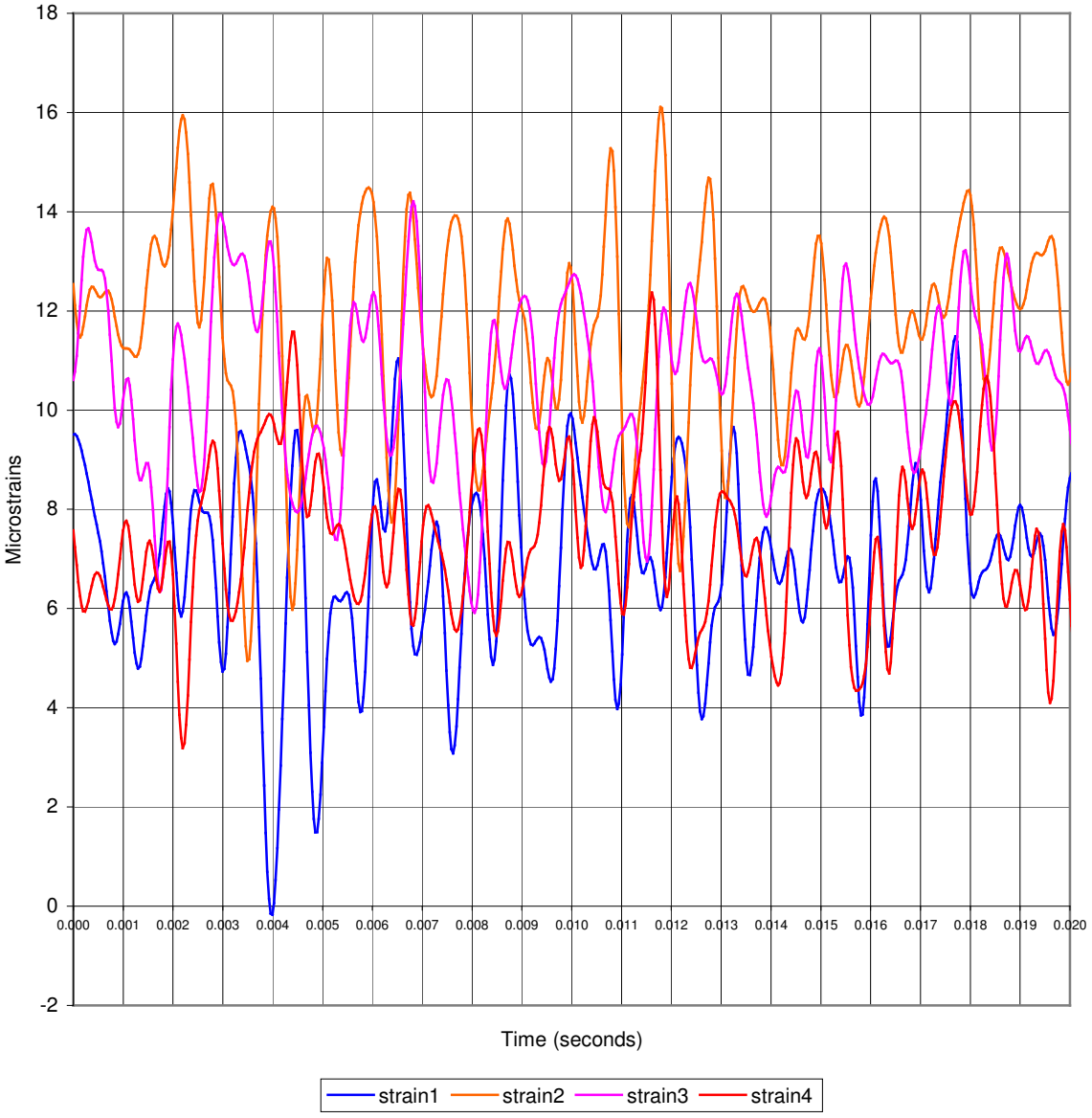

Figure 4.8: Bracket Impact Strain Gages Filtered to 2500Hz

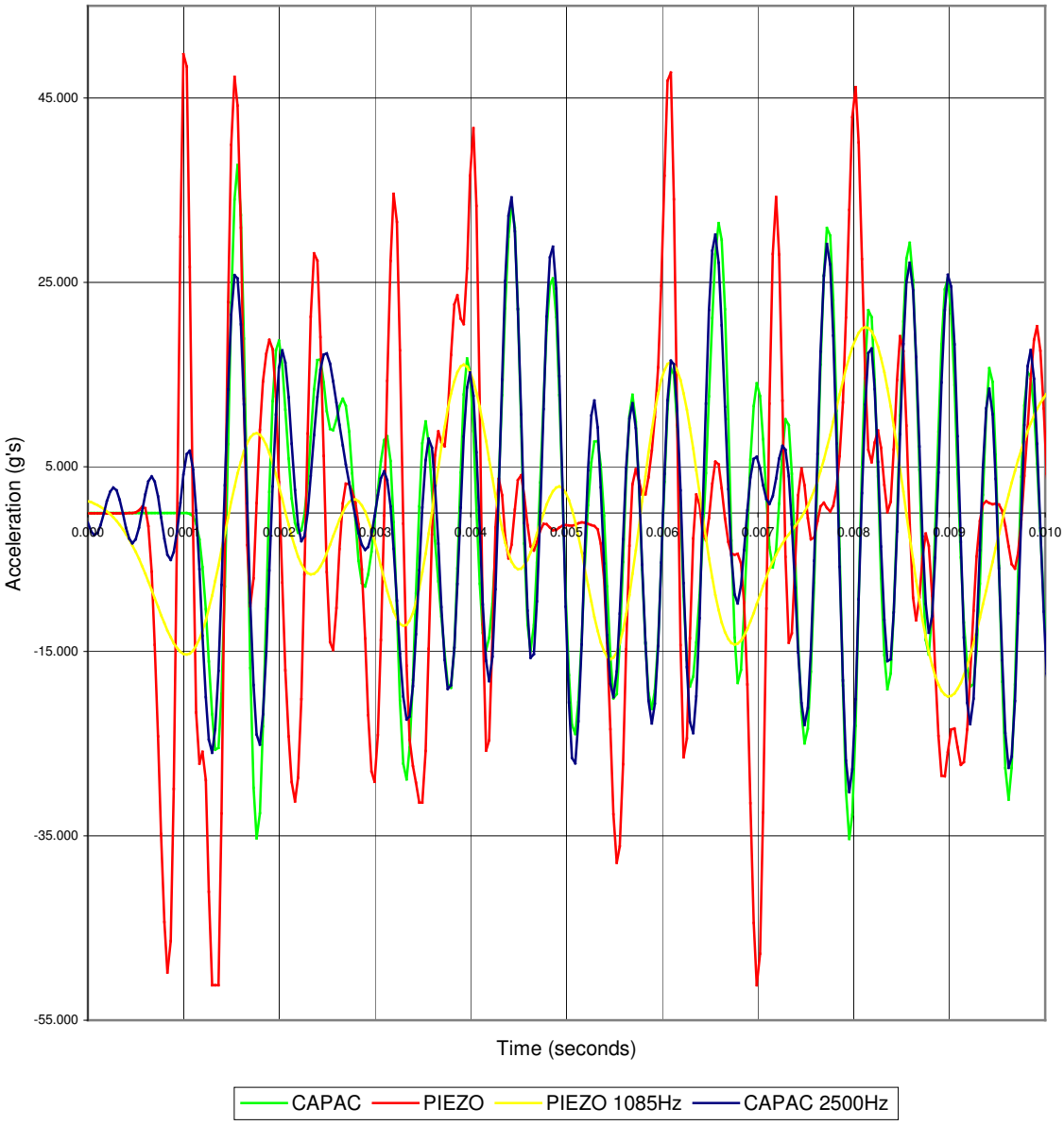

Figure 4.9: Top Impact Accelerometer Data

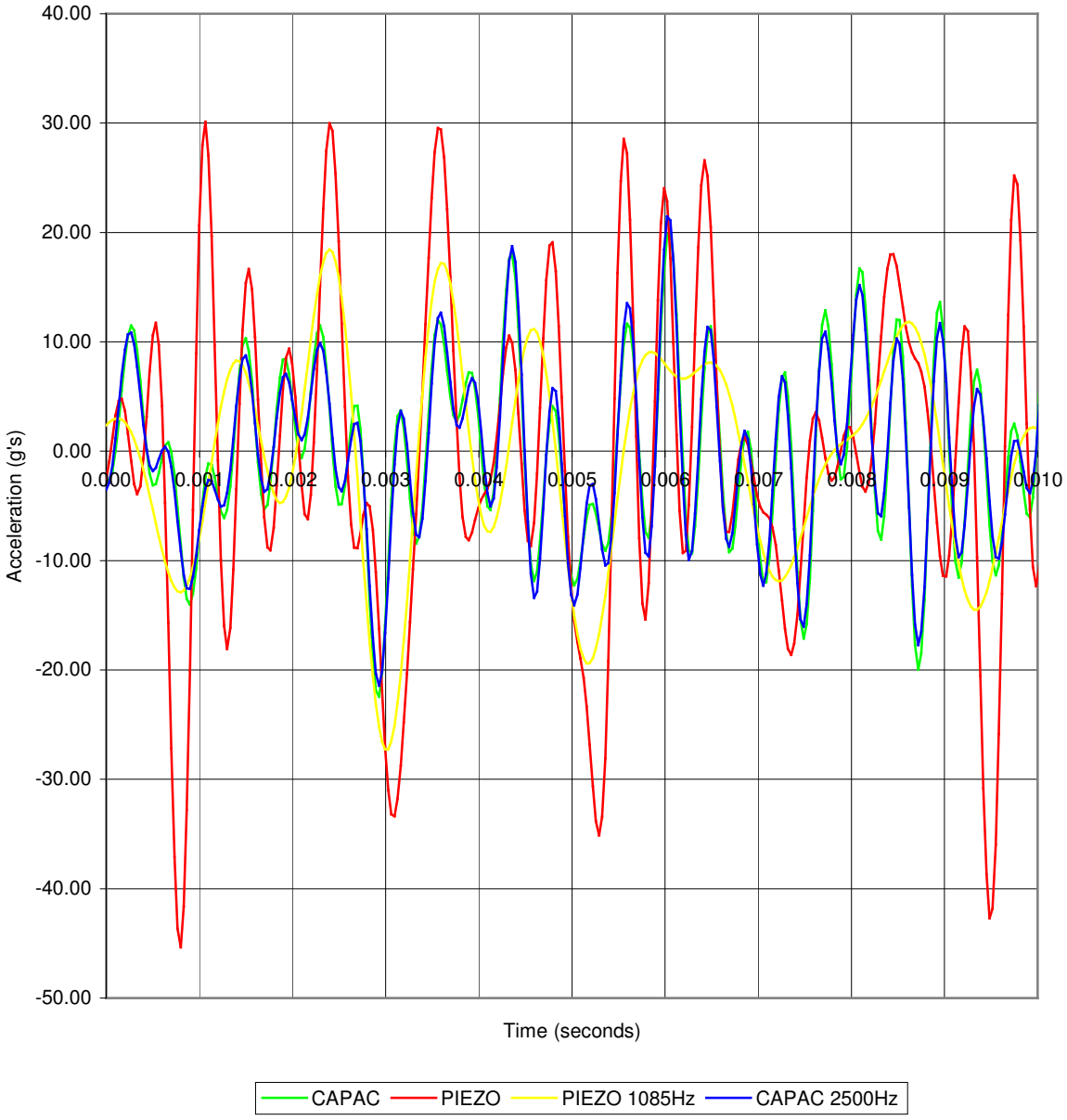

Figure 4.10: Center Impact Accelerometer Data

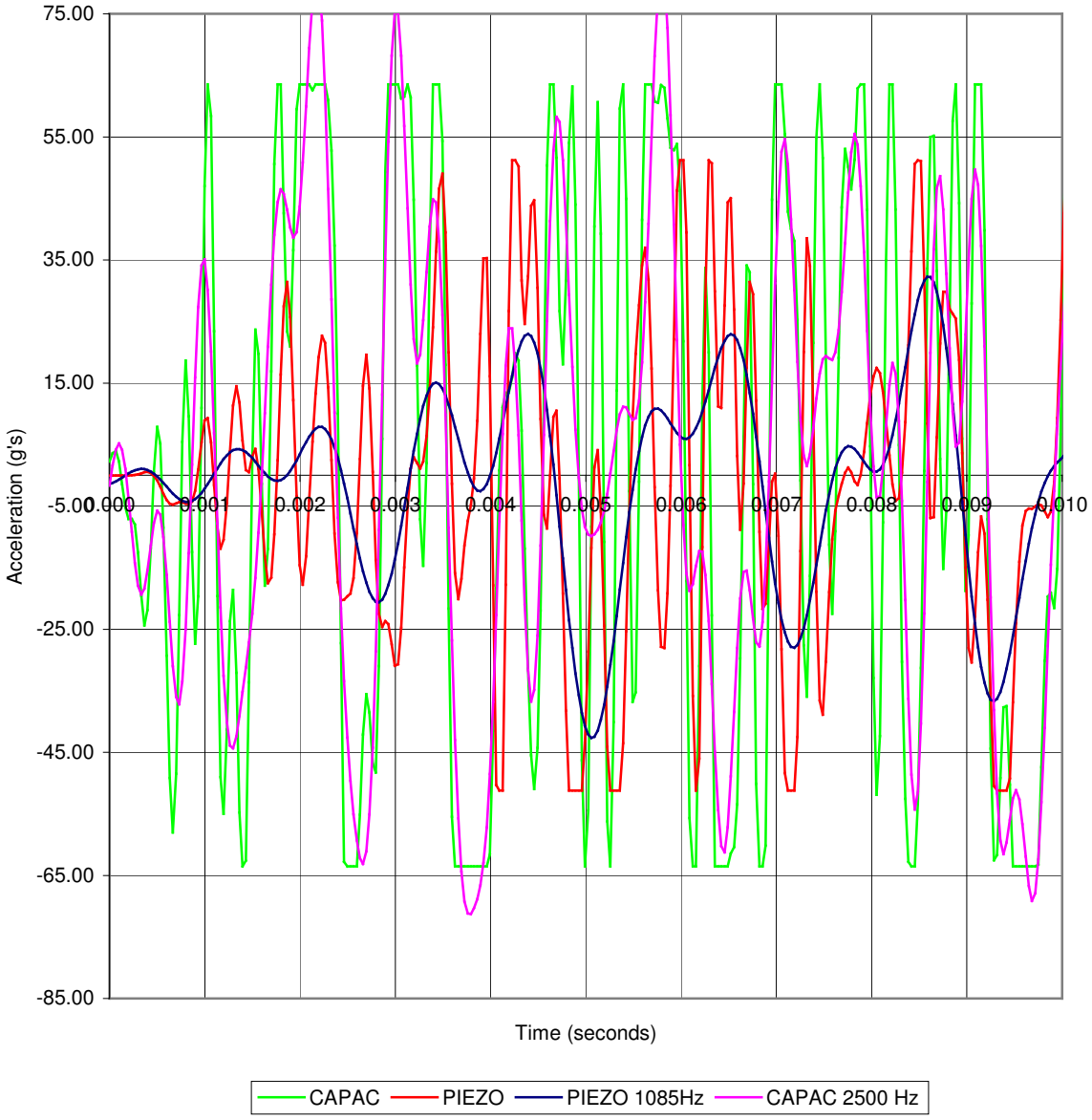

Figure 4.11: Bracket Impact Accelerometer Data

Chapter 5 Summary & Recommendations

5.1 Summary

Methods of non-destructive testing have become necessary in identifying unknown foundations. Developing instrumentation is vital to such an endeavor. In this thesis, strain gages and accelerometers were examined in the arena of impact loading of concrete pilings. Measured strains identified stress wave velocities and direction, which was used to determine pile length. Axial loading produced stress waves consistent with compression wave propagation. Surface and shear waves were prevalent under flexural bending associated with lateral impacts. Both the capacitive and piezoelectric accelerometers were successful in capturing data in all trial and testing scenarios.

5.2 Recommendations

There were several types of impacts observed (i.e. top, side & bracket). The best performance was from the top. A method to deliver pure axial loading to the side of a piling would be ideal. The first recommendation is, instead of a hammer, a weighted ring or sleeve wrapped around a piling may be dropped onto a bracket fastened to the side. The weight of the ring may vary depending on projected pile depth or stiffness of the soil.

The use of multiple gages helped determine wave velocities and direction. It is recommended that gages be spread apart as far as possible on the same side of the piling. The further apart, the more accurate it is when calculating wave speed. It took several

hours for the strain gage epoxy to set. It might be more cost effective to use a gage that fastens quicker and is reusable.

Accelerometers that are used as trigger mechanisms should be set to activate under both positive and negative accelerations. It is important to capture an adequate amount of pre-trigger time. Total sampling time can be estimated based on wave speed through a projected pile depth. When setting a sampling rate, consider the number of data points needed to do a Fourier transform.

References

1. U. Meier and R. Betti, "Recent Advances in Bridge Engineering," Printing Office Columbia University New York, 1997.

2. Baldev Raj, T. Jayakumar and M. Thavasimuthu, "Practical Non-Destructive Testing," Narosa Publishing House, 2002.

3. Federal Highways Administration – Geophysical Imaging Resource Website<http://www.cflhd.gov/agm/engApplications/BridgeSystemSubstructure/212BoreholeNondestMethods.htm >Last Accessed on 15 March 2007.

4. Federal Highways Administration - Unknown Foundation Summit, Lakewood, Colorado, November 15-16, 2005.

5. Mullins G., Kranc S., Johnson K., Stokes M., Winters D., "Thermal Integrity Testing of Drilled Shafts," University of South Florida, 2007.

6. Northwestern University Infrastructure Technology Institute Website<http://www.iti.northwestern.edu/technology/midwest/november2000/newy ork/html/slide6.html>Last Accessed 15 March 2007.

7. Petros P. Xanthakos, "Bridge Substructure and Foundation Design," Prentice Hall PTR, 1995.

Appendices

Appendix A Results from Laboratory Trials

Included in this appendix are trial impacts conducted in the lab. Piezoelectric and capacitive accelerometers were both located on the midline bracket. Impact was created with a 12-ounce hammer. Strikes were made to the top and mid-line bracket. Impacts were also on the lateral face of the pile midway and at the bottom.

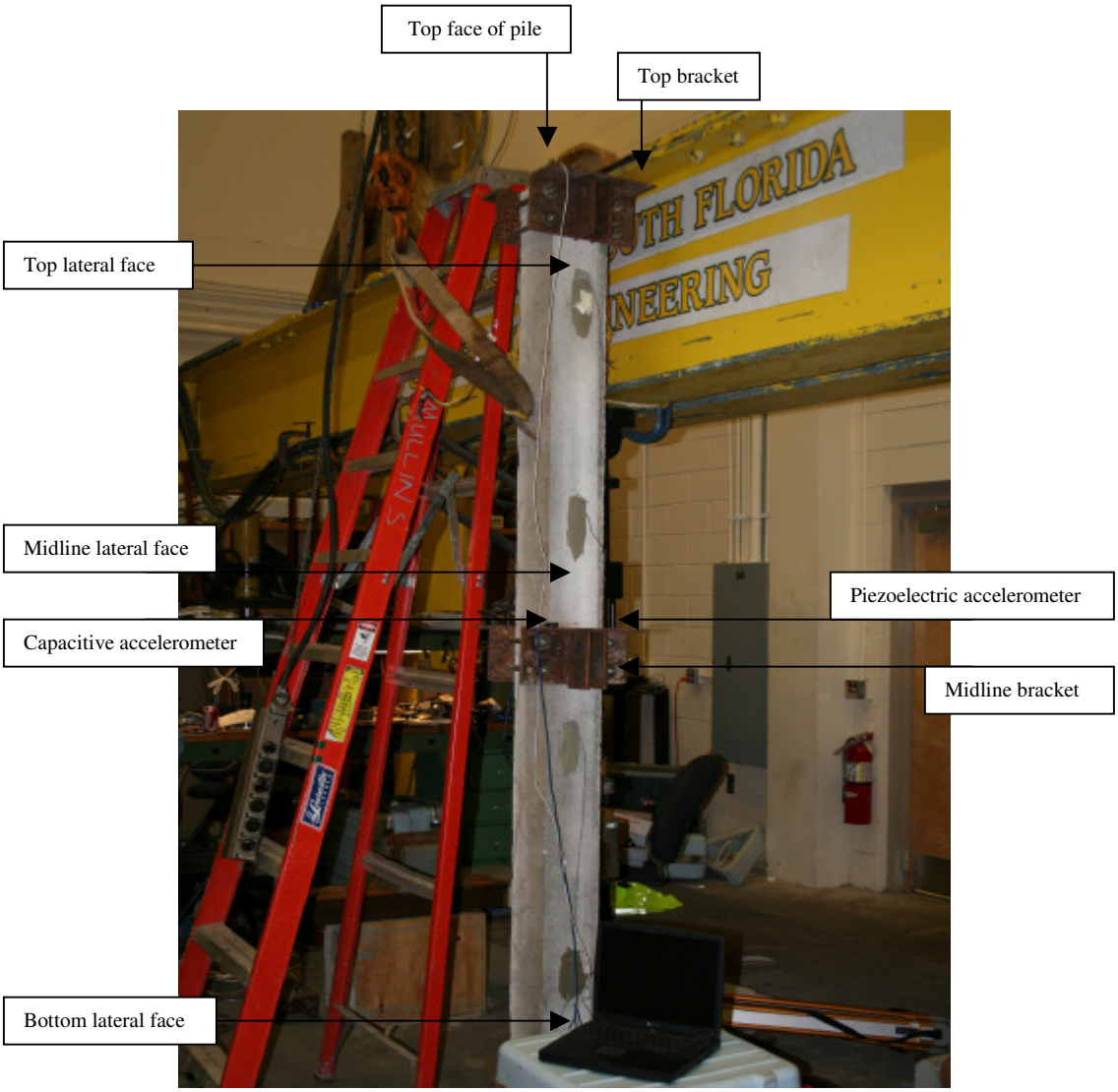

Figure A.1: Laboratory 6"x 6" Pile Accelerometer Placement

Appendix A (Continued)

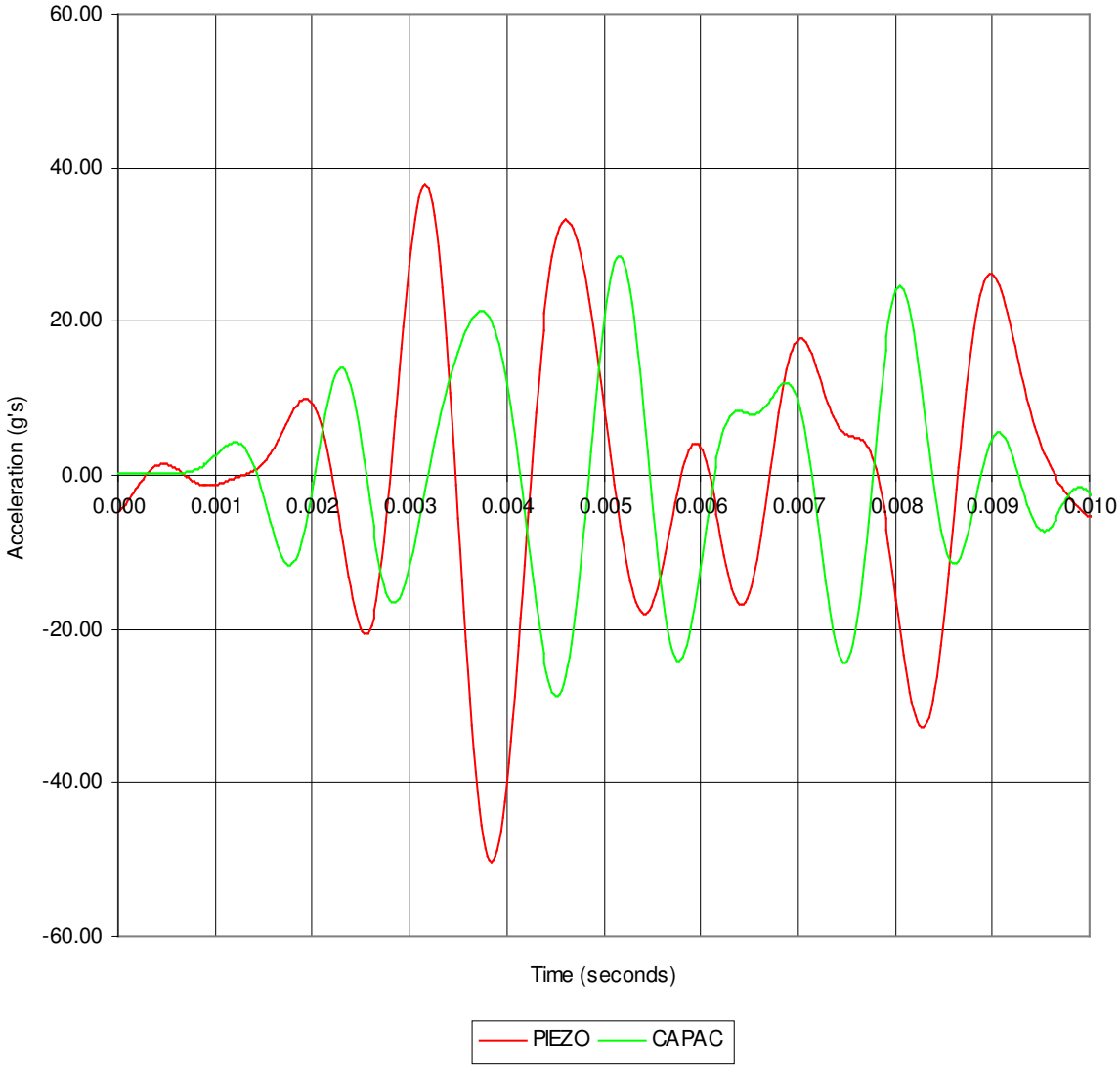

Figure A.2: Midline Bracket Impact Accelerations Trial 001

Appendix A (Continued)

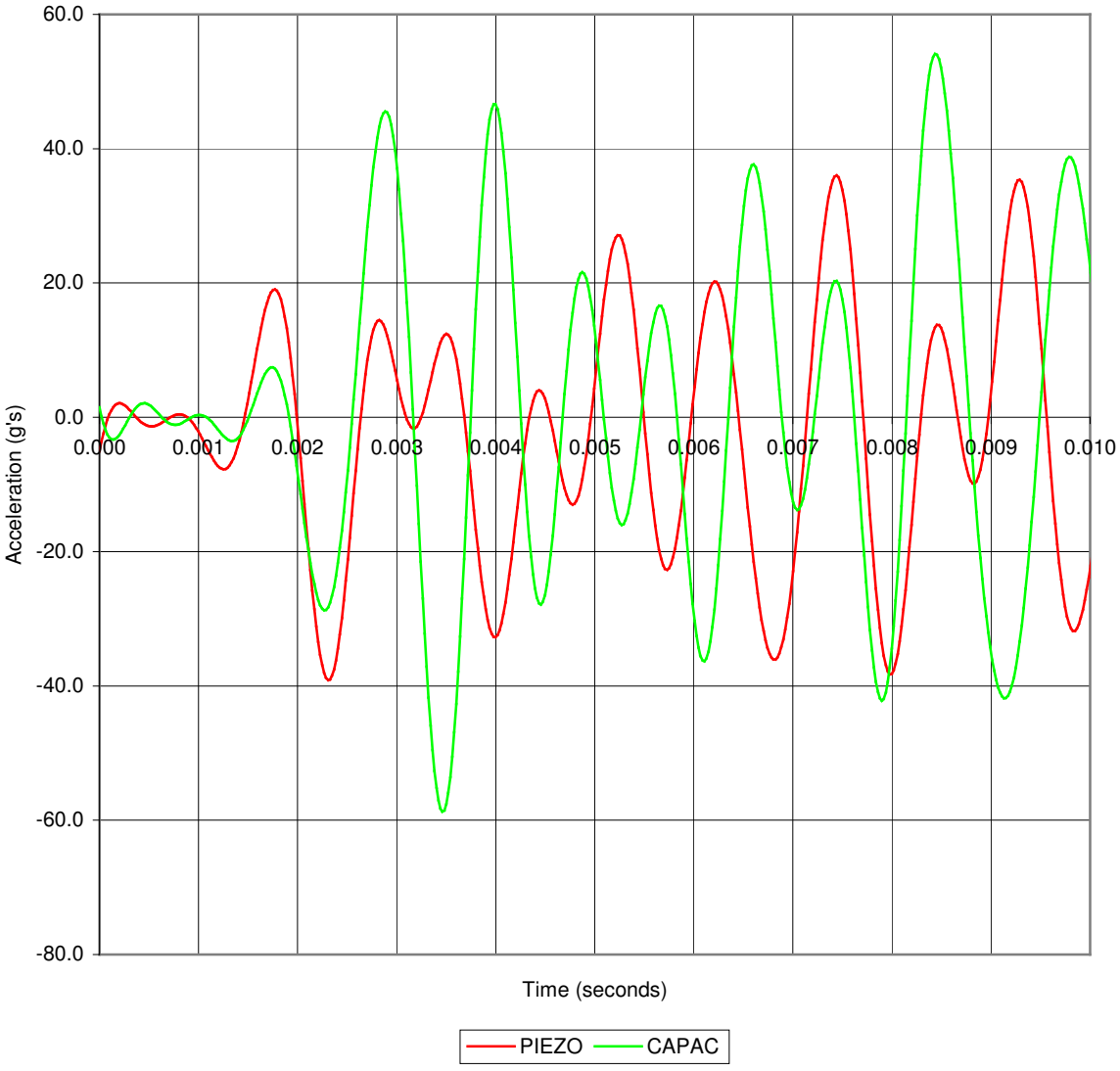

Figure A.3: Midline Bracket Impact Accelerations Trial 002

Appendix A (Continued)

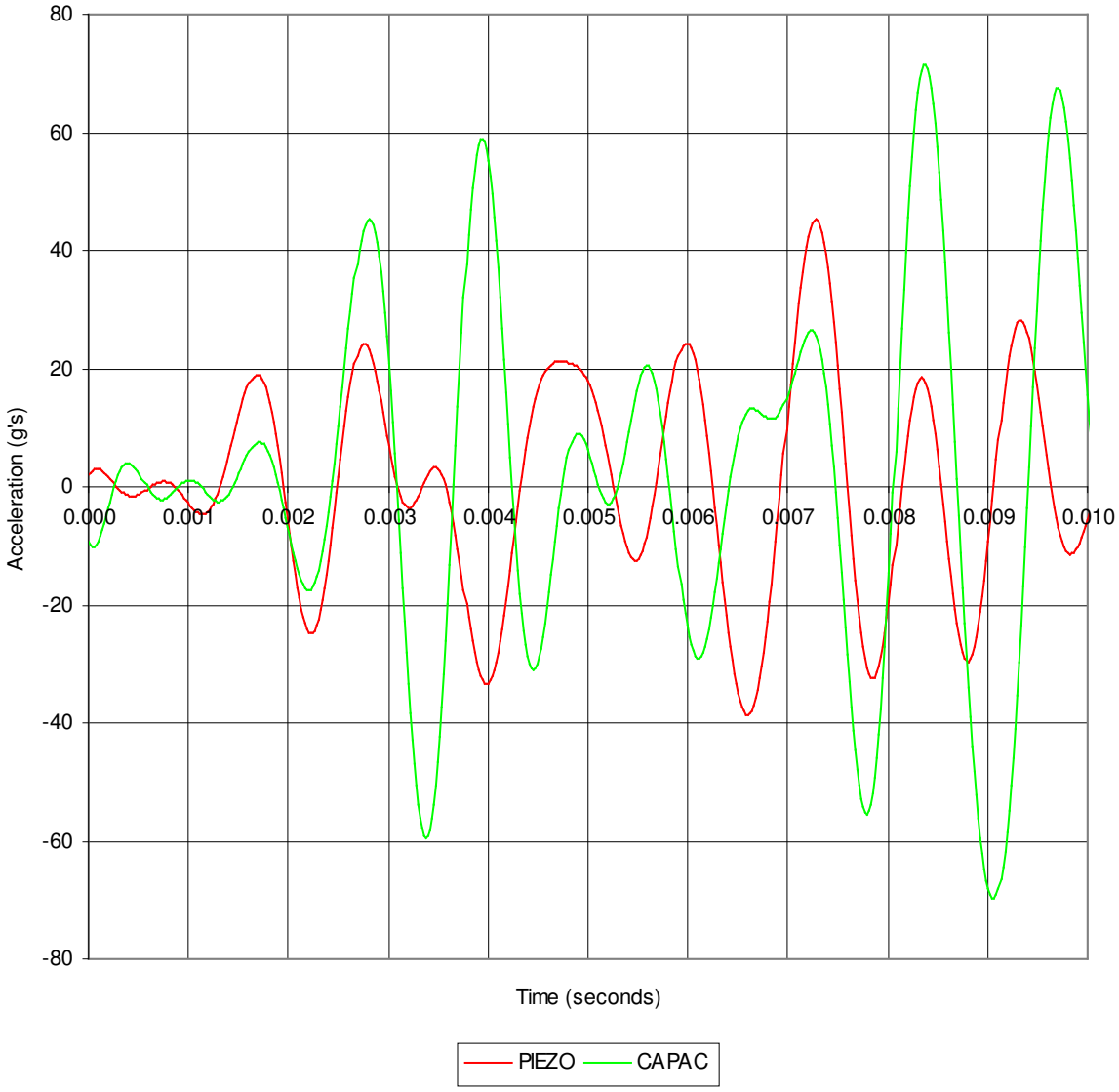

Figure A.4: Midline Bracket Impact Accelerations Trial 003

Appendix A (Continued)

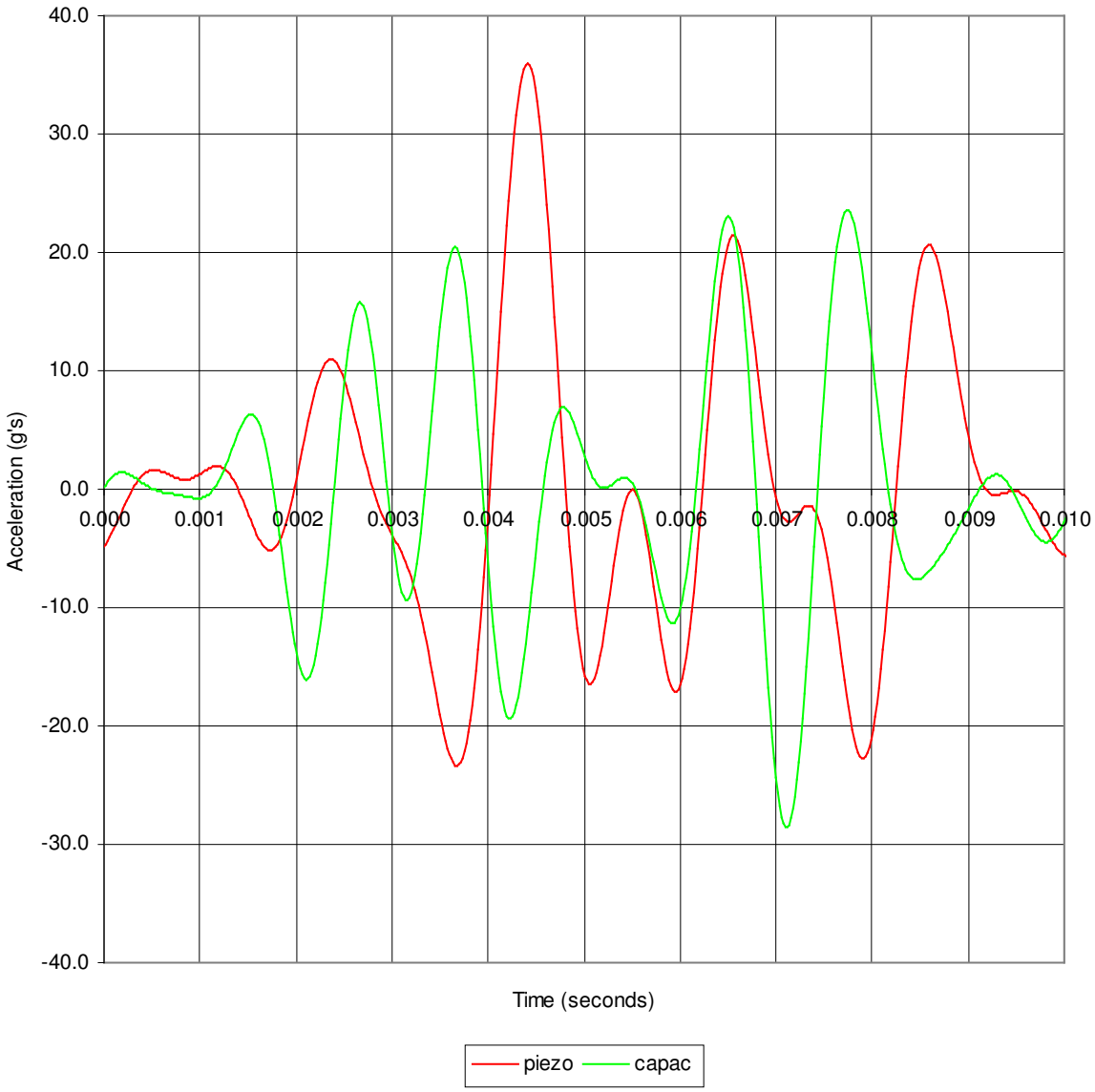

Figure A.5: Bottom Lateral Side Impact Accelerations Trial 004

Appendix A (Continued)

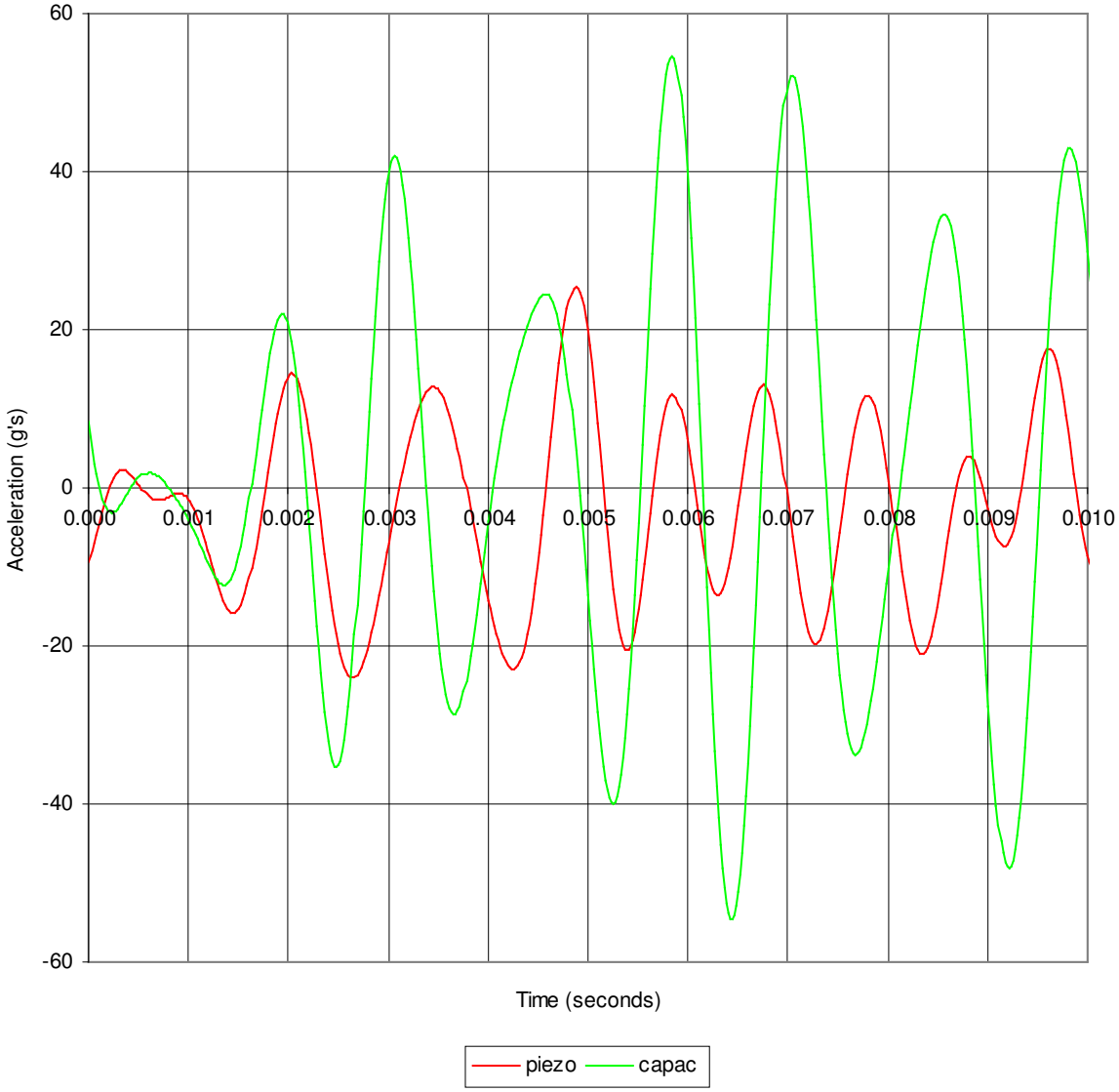

Figure A.6: Top Bracket Impact Accelerations Trial 005

Appendix A (Continued)

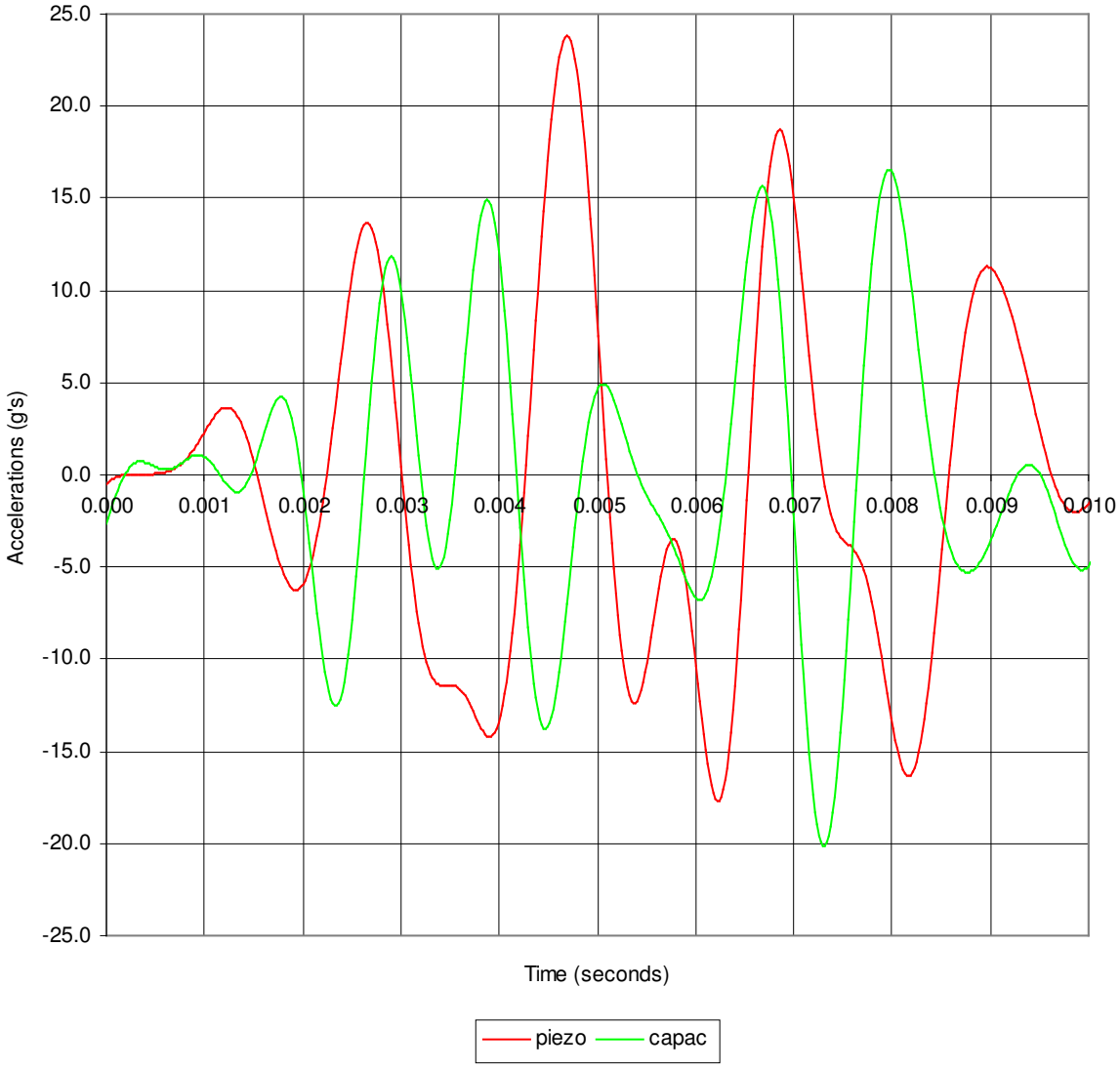

Figure A.7: Bottom Lateral Side Impact Accelerations Trial 006

Appendix A (Continued)

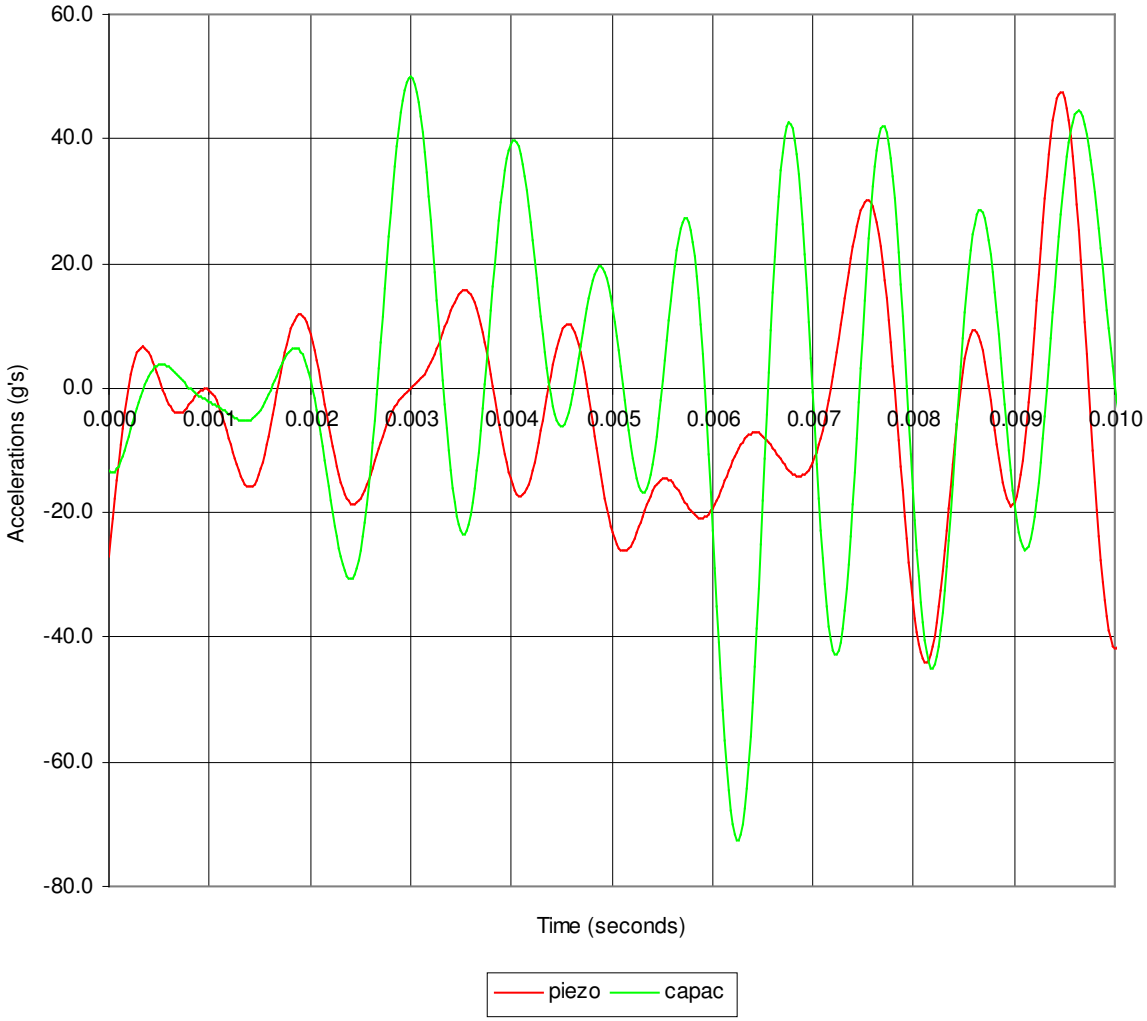

Figure A.8: Midline Bracket Impact Accelerations Trial 007

Appendix A (Continued)

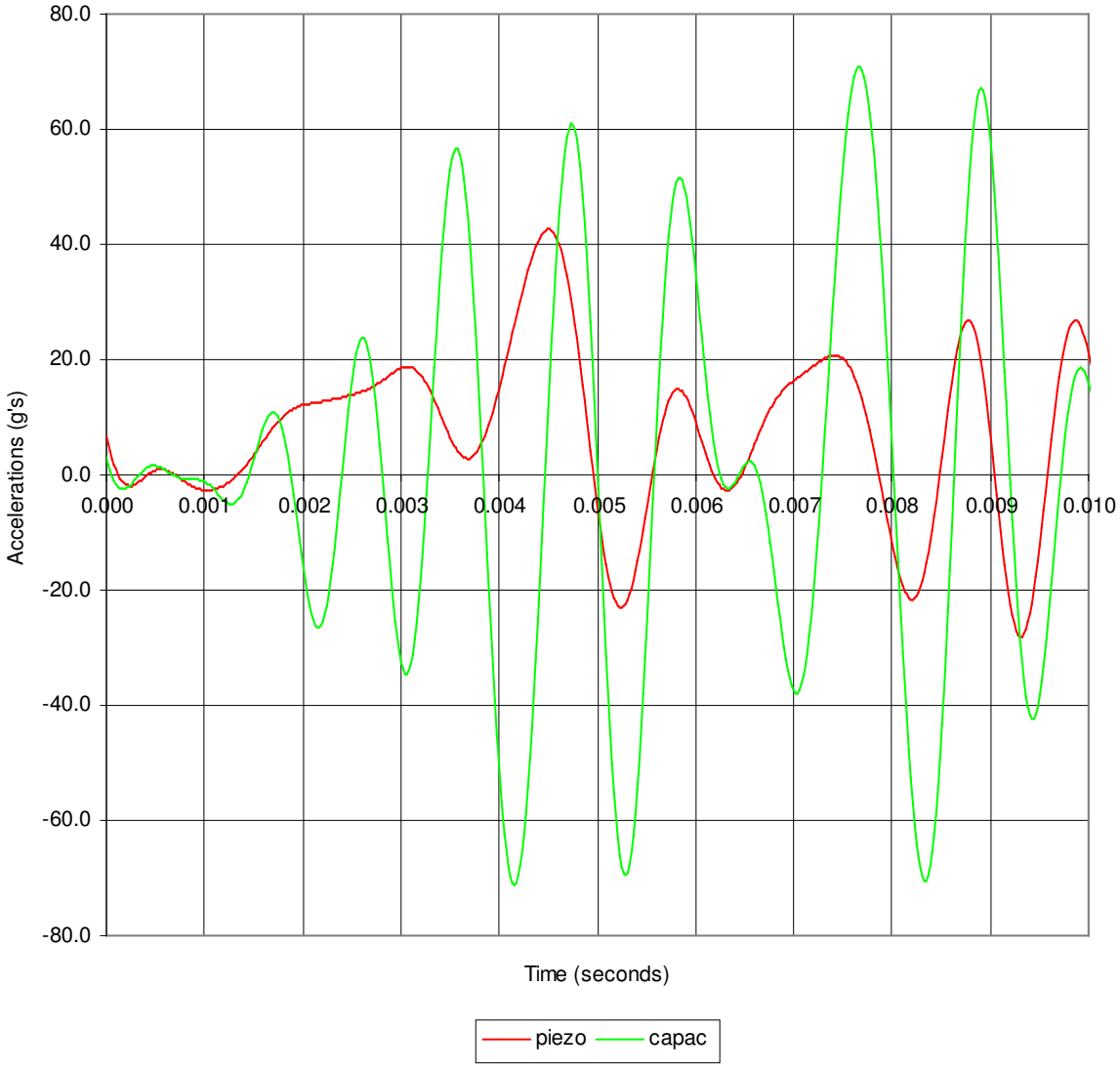

Figure A.9: Top Lateral Side Impact Accelerations Trial 008

Appendix A (Continued)

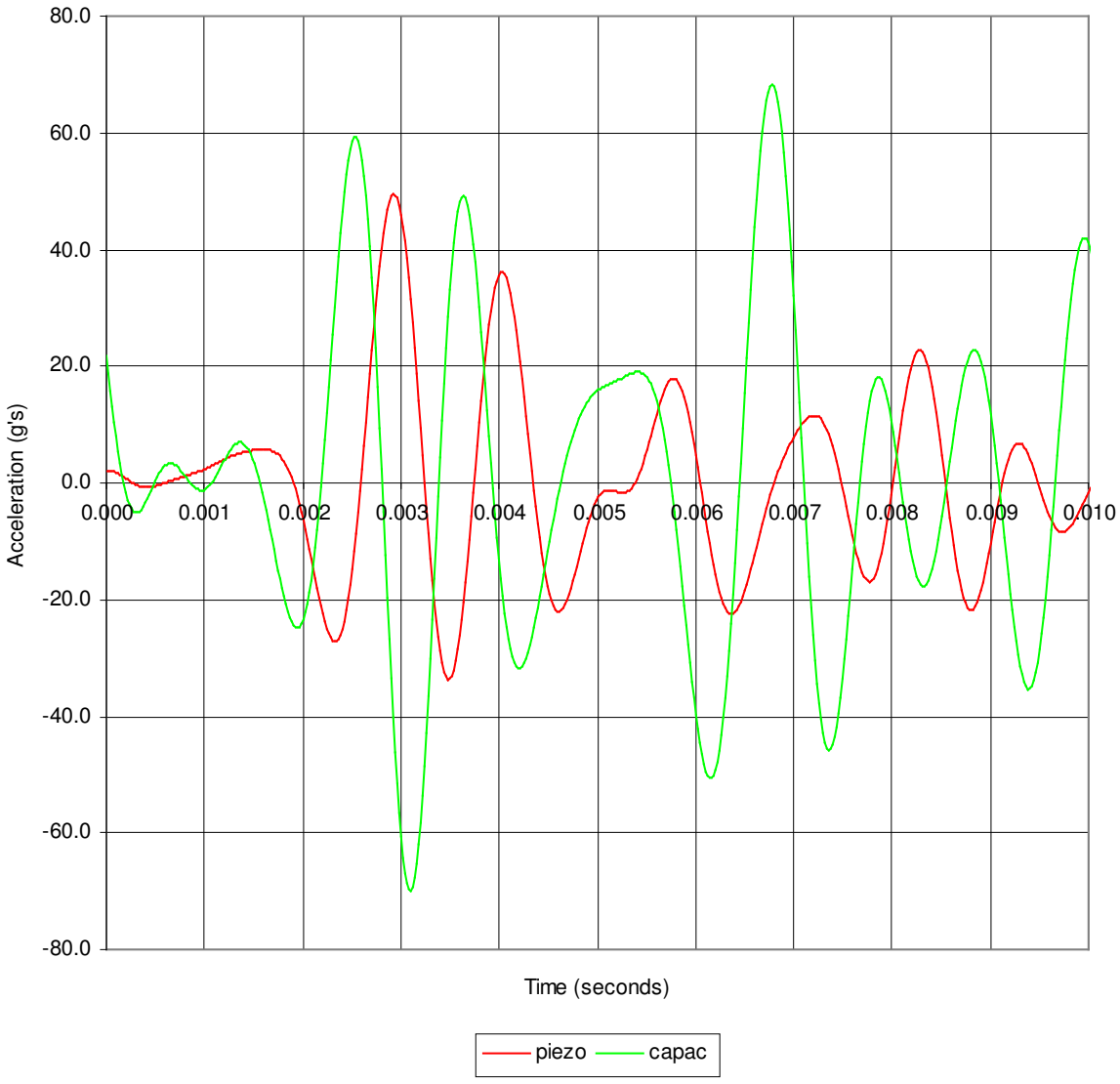

Figure A.10: Bottom Lateral Side Impact Accelerations Trial 009

Appendix A (Continued)

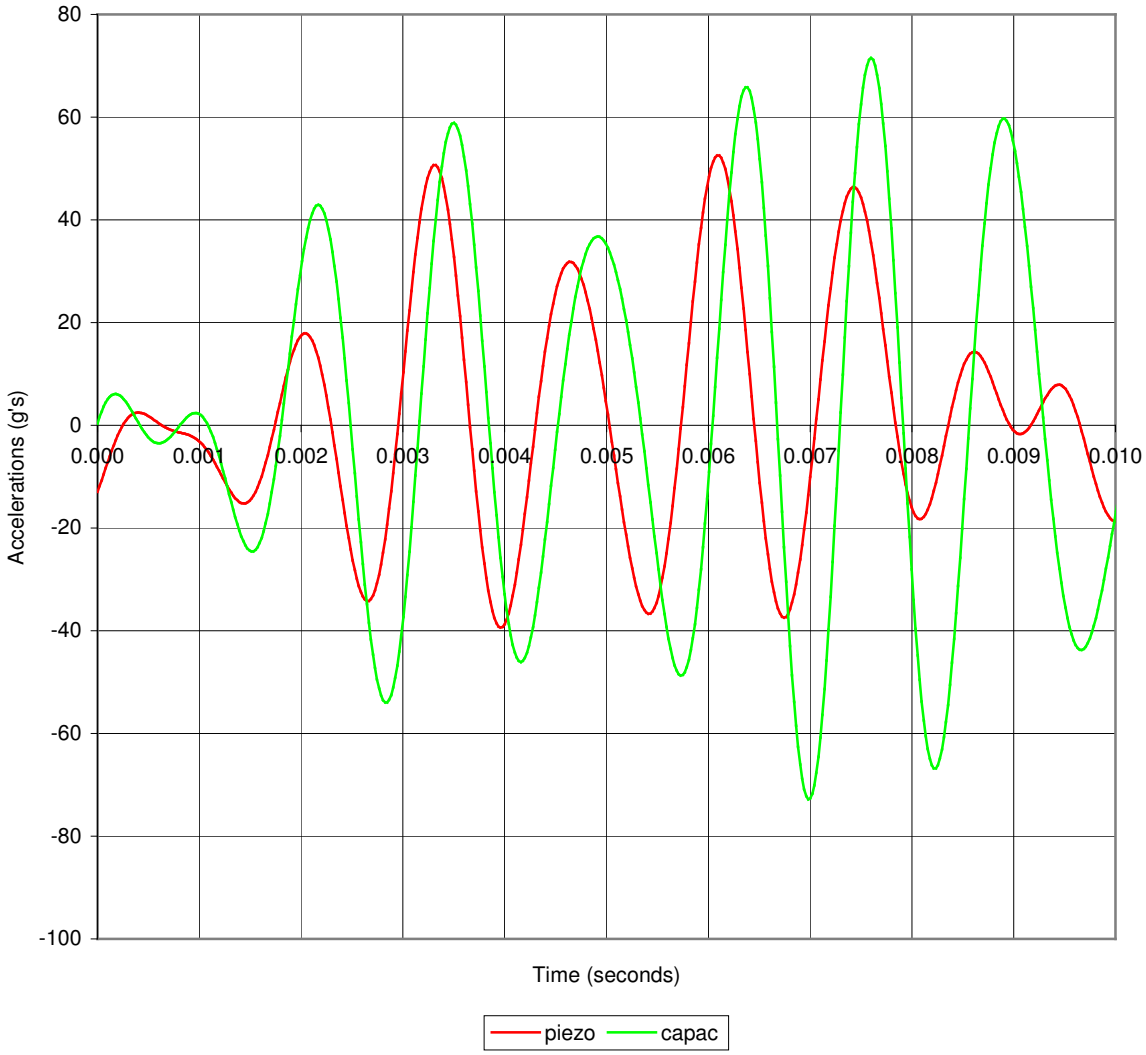

Figure A.11: Top of Piling Impact Accelerations Trial 010

Appendix A (Continued)

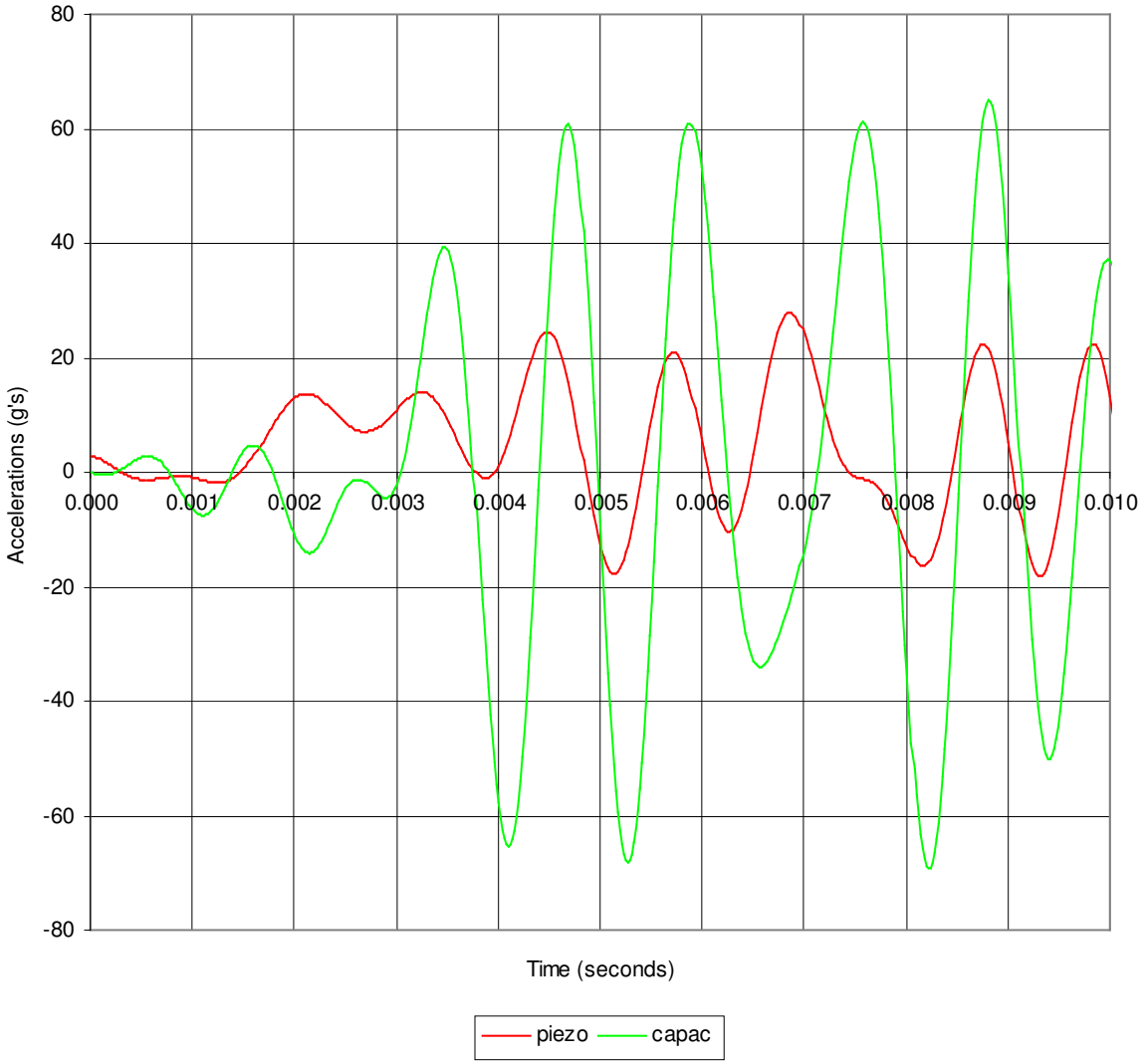

Figure A.12: Top Lateral Side Impact Accelerations Trial 011

Appendix A (Continued)

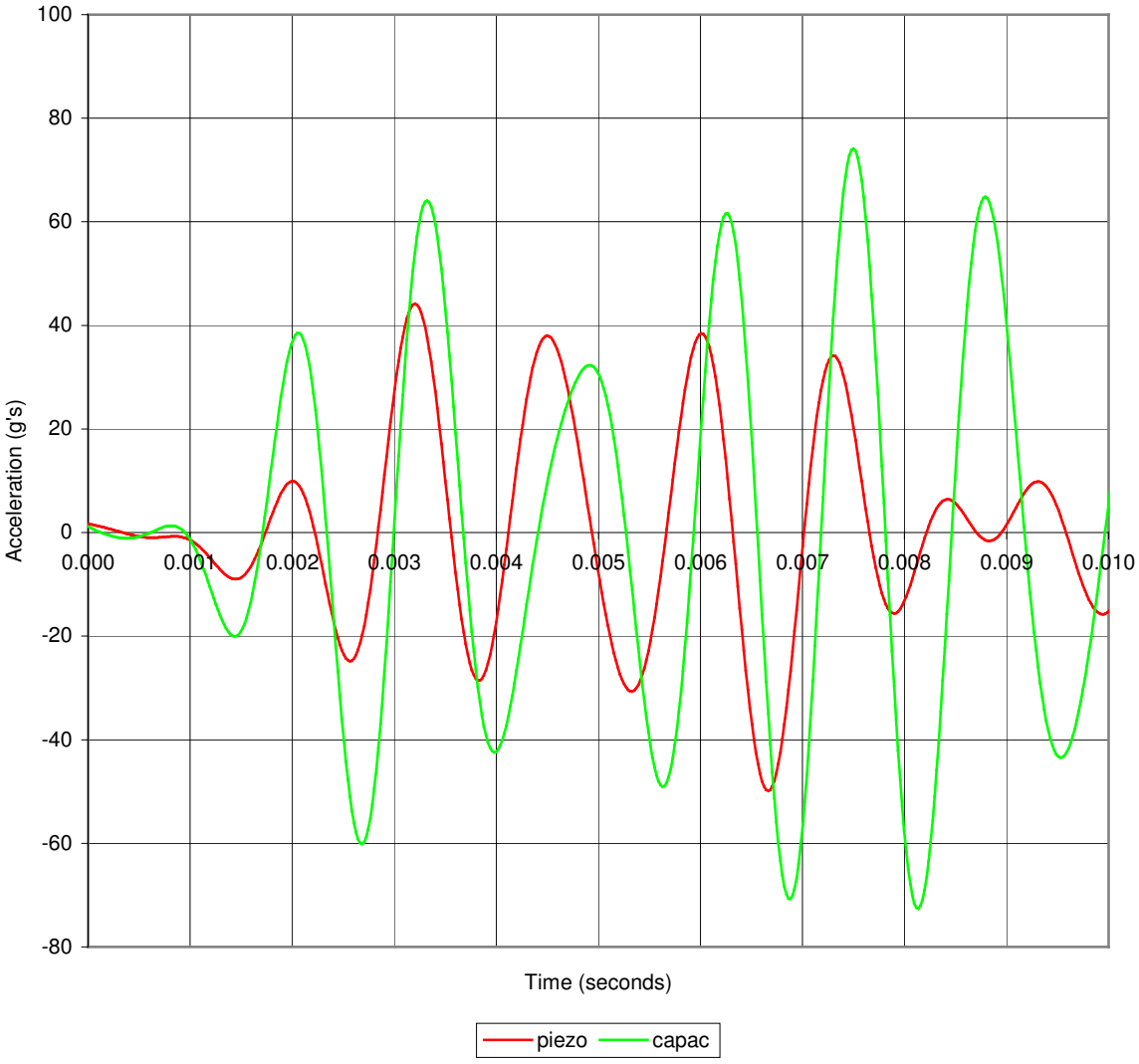

Figure A.13: Top of Piling Impact Accelerations Trial 012

Appendix A (Continued)

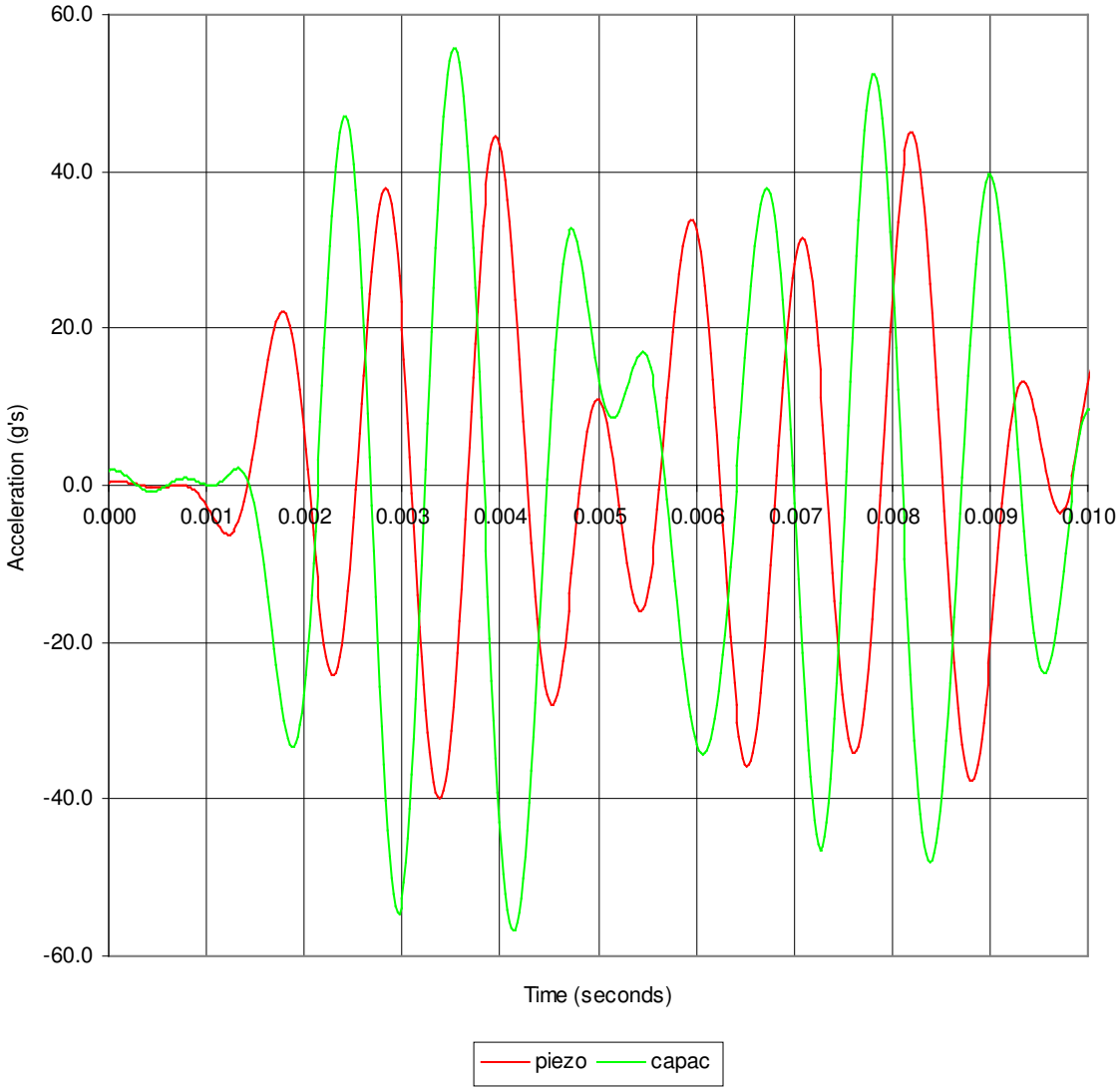

Figure A.14: Midline Lateral Side Impact Accelerations Trial 013

Appendix A (Continued)

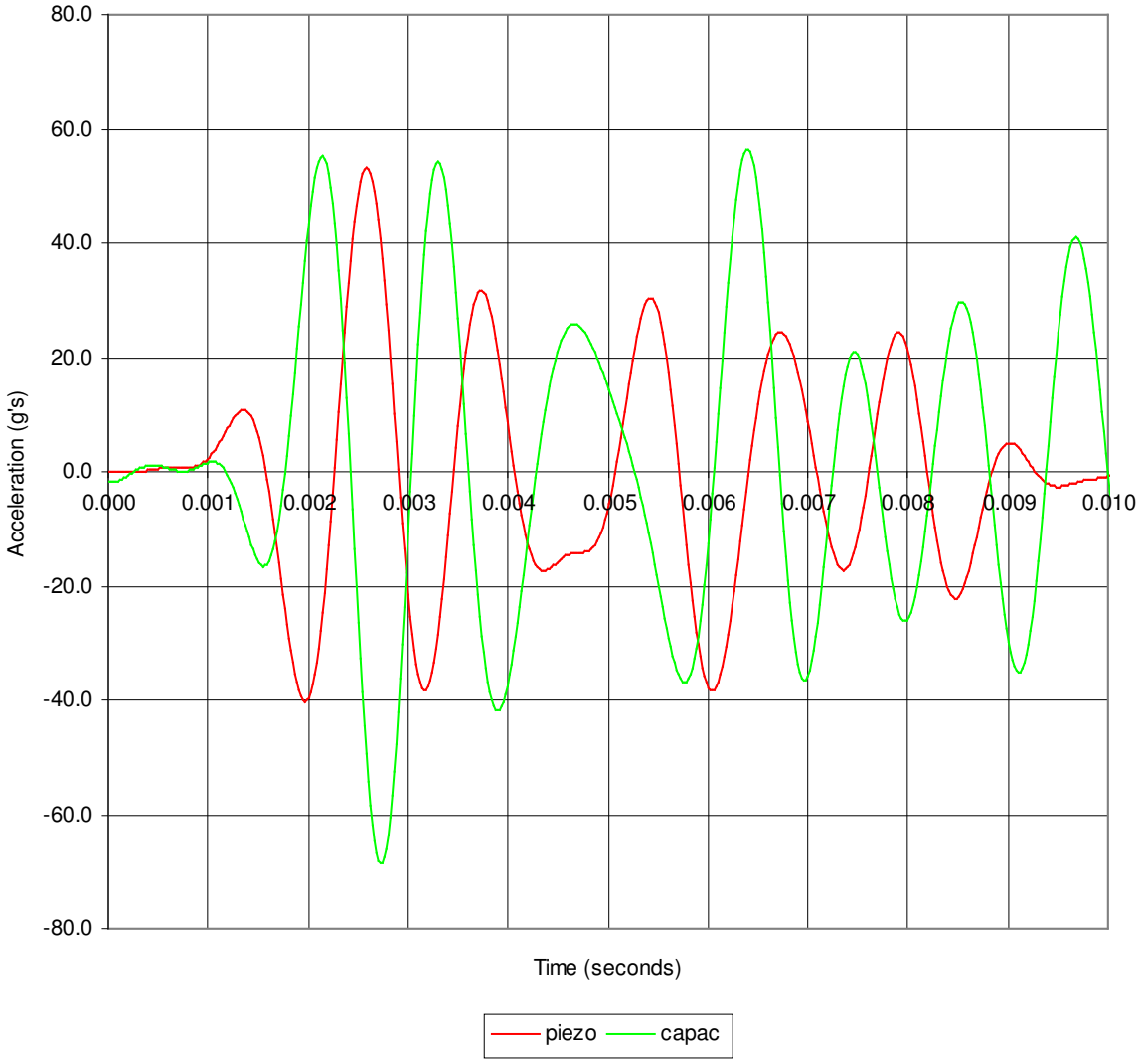

Figure A.15: Bottom Lateral Side Impact Accelerations Trial 014

Appendix A (Continued)

Strain gages were included in the following trial. The Piezoelectric accelerometer was located on the top bracket. The capacitive accelerometer was located on the midline bracket. Impact was created with a 12-ounce hammer strike to the top face of the pile.

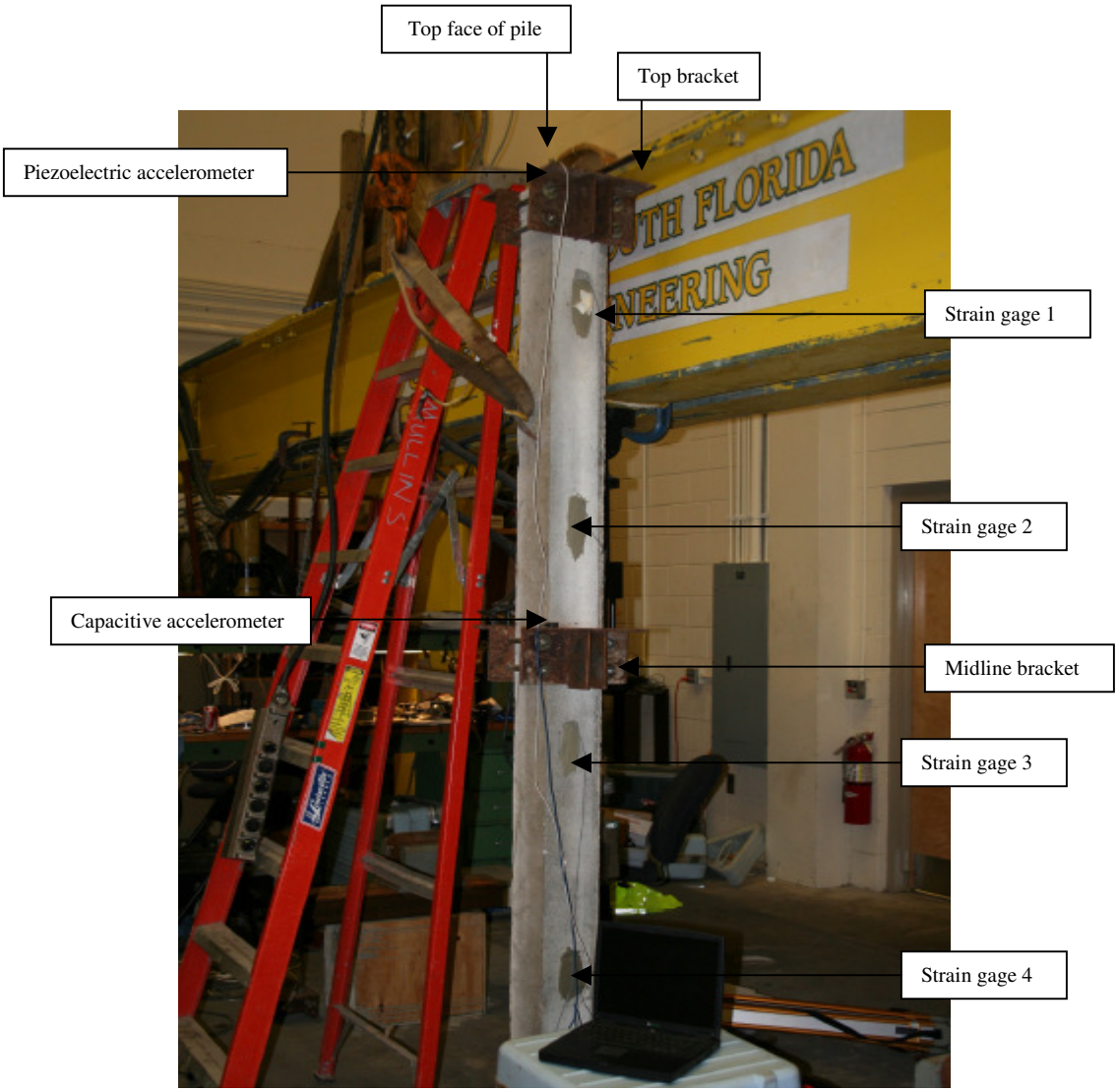

Figure A.16: Laboratory 6"x 6" Pile Accelerometer and Strain Gage Placement

Appendix A (Continued)

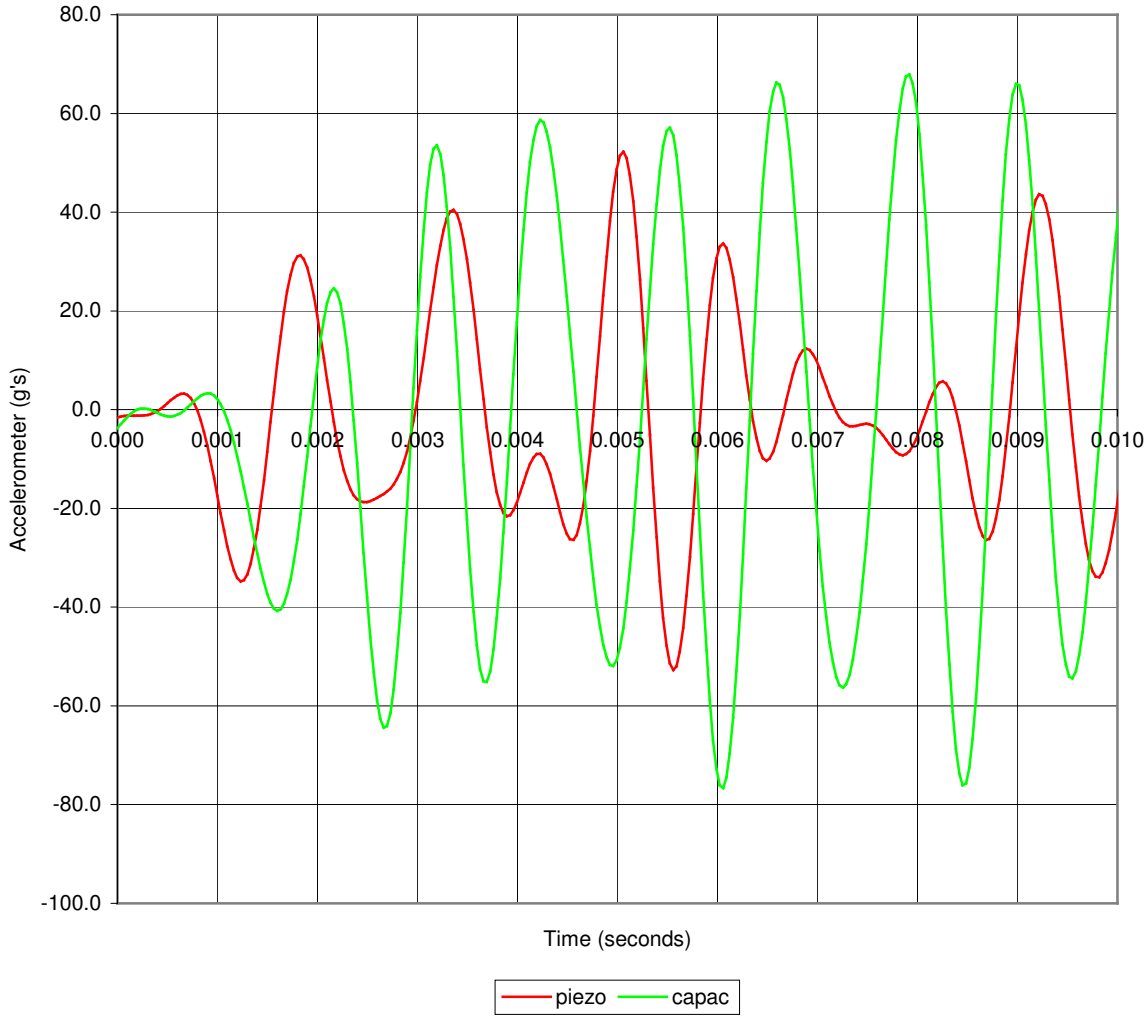

Figure A.17: Top of Piling Impact Accelerations Trial 015

Appendix A (Continued)

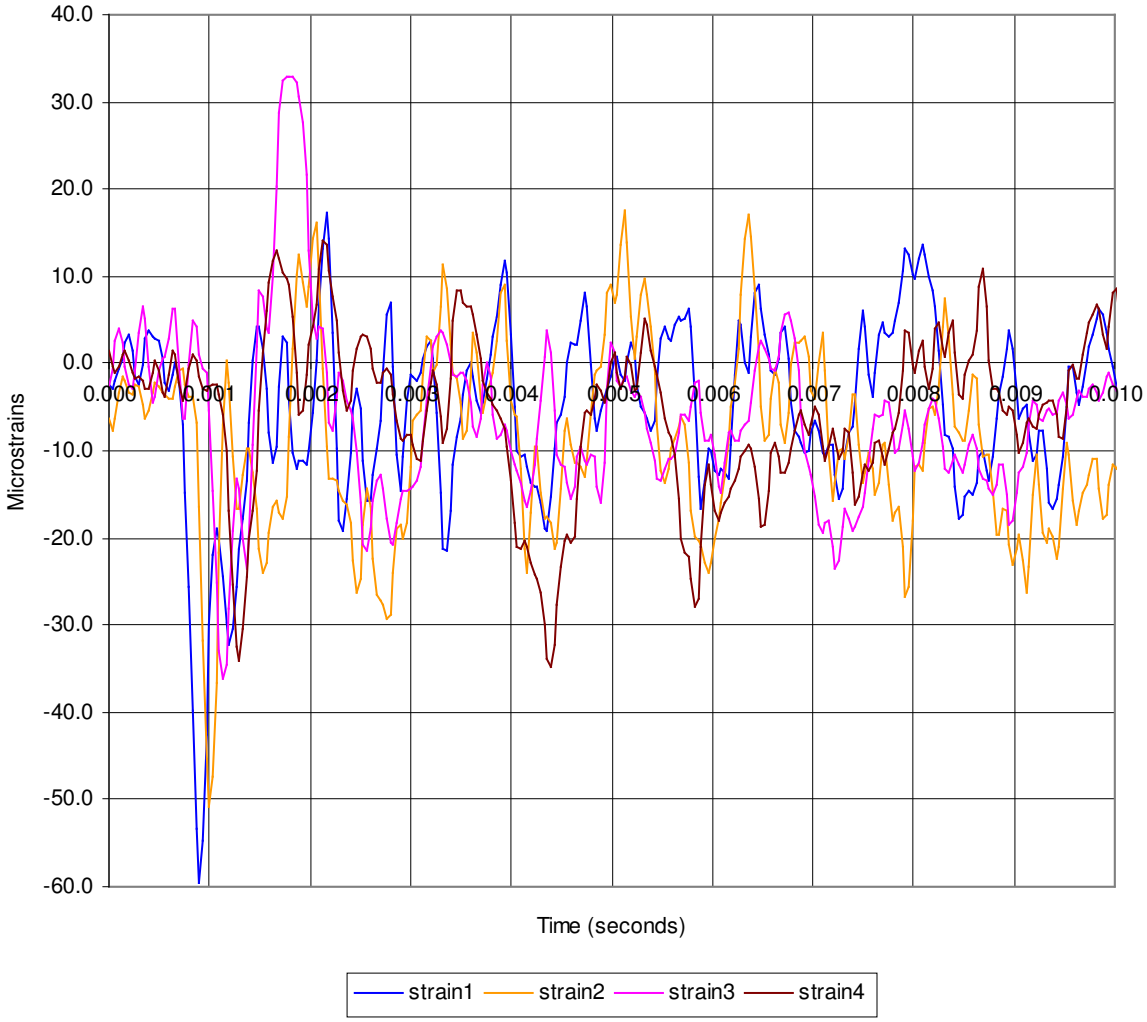

Figure A.18: Top of Piling Impact Strain Data Trial 015

Appendix B Results from Field Testing

Included in this appendix are field studies performed on a 12”x 12”x 40’ pre-stressed concrete piling. Strain gages were included in the following data. The Piezoelectric accelerometer was located on the top bracket. The capacitive accelerometer was located on the midline bracket. Impact was created with a 12-ounce hammer strike to the top, lateral side and mounted bracket of the pile.

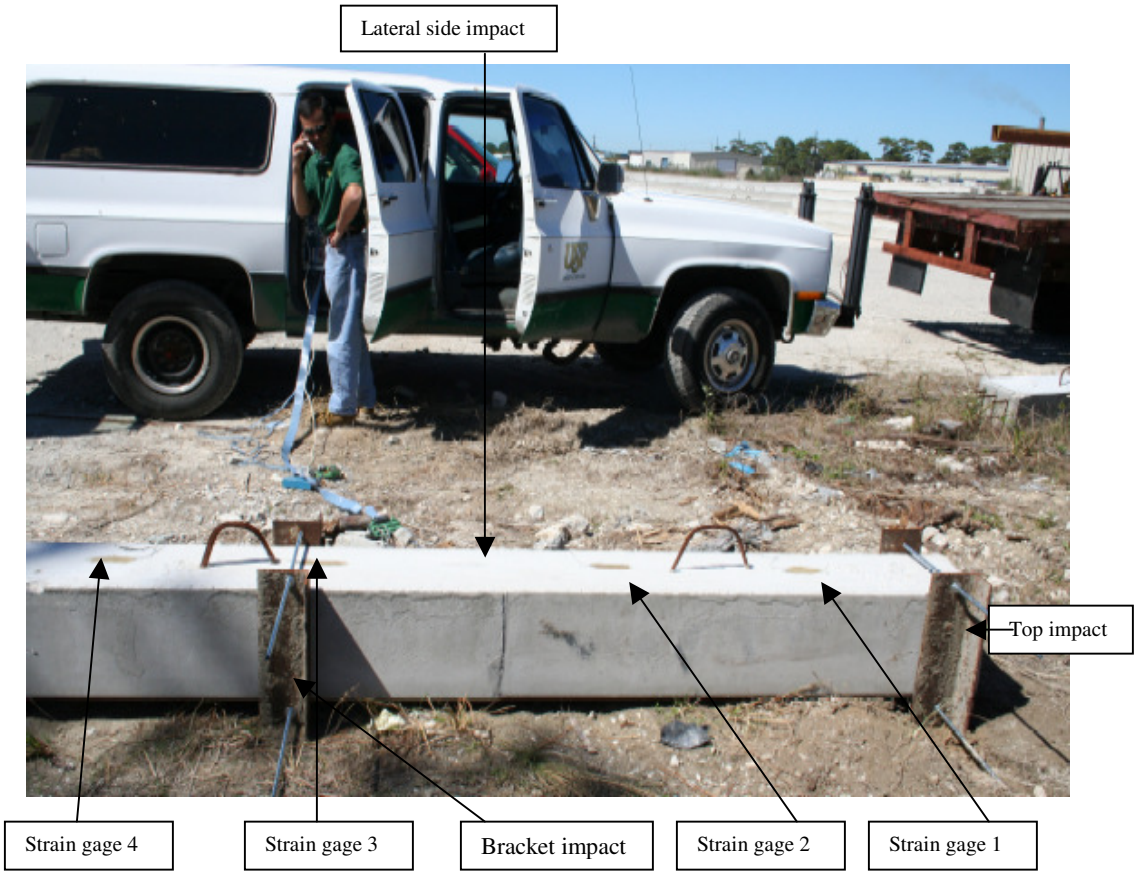

Figure B.1: Accelerometer and Strain Gage Placement 12”x 12”x 40’ Piling

Appendix B (Continued)

Figure B.2: Top of Piling Impact Accelerations - Test 2

Appendix B (Continued)

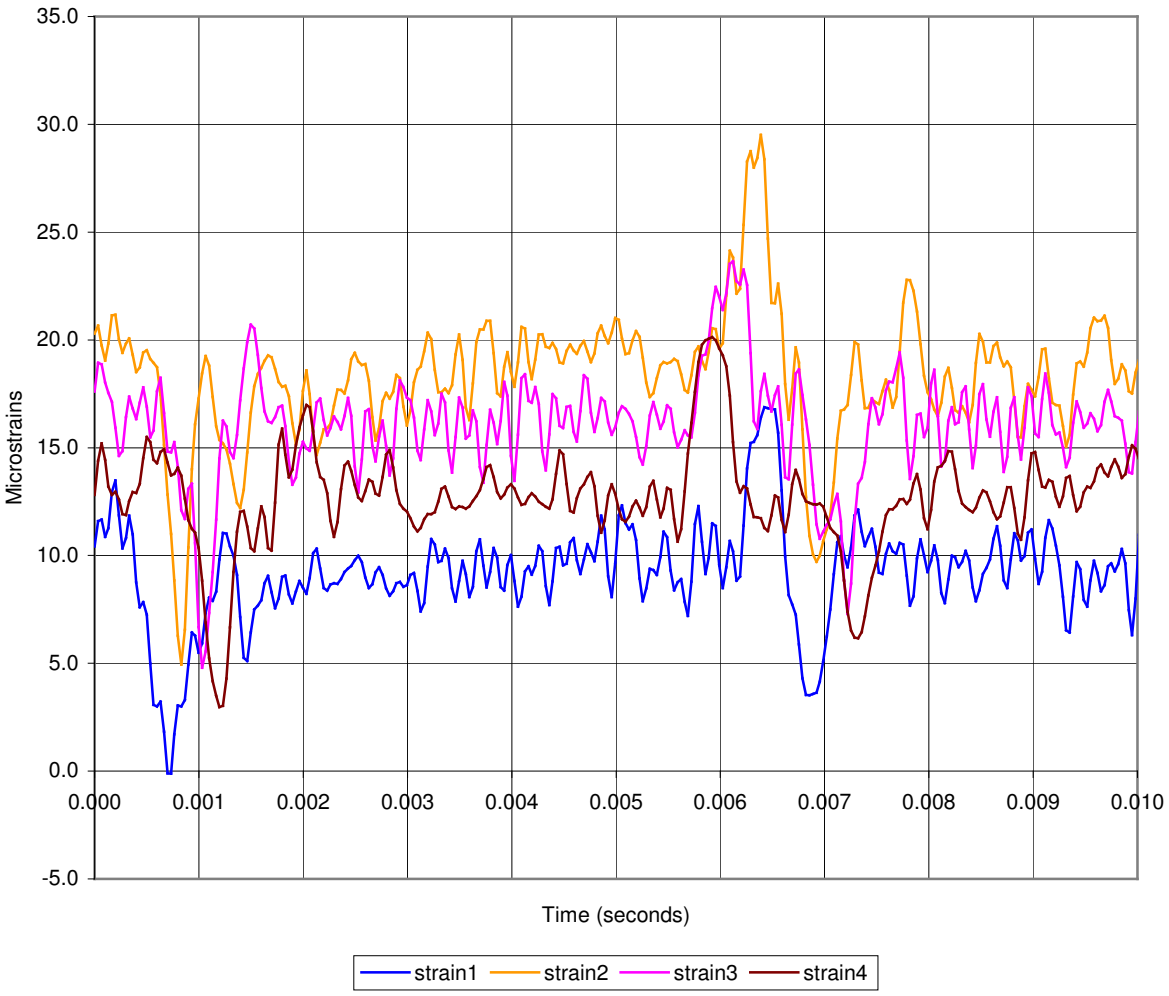

Figure B.3: Top of Piling Impact Strains - Test 2

Appendix B (Continued)

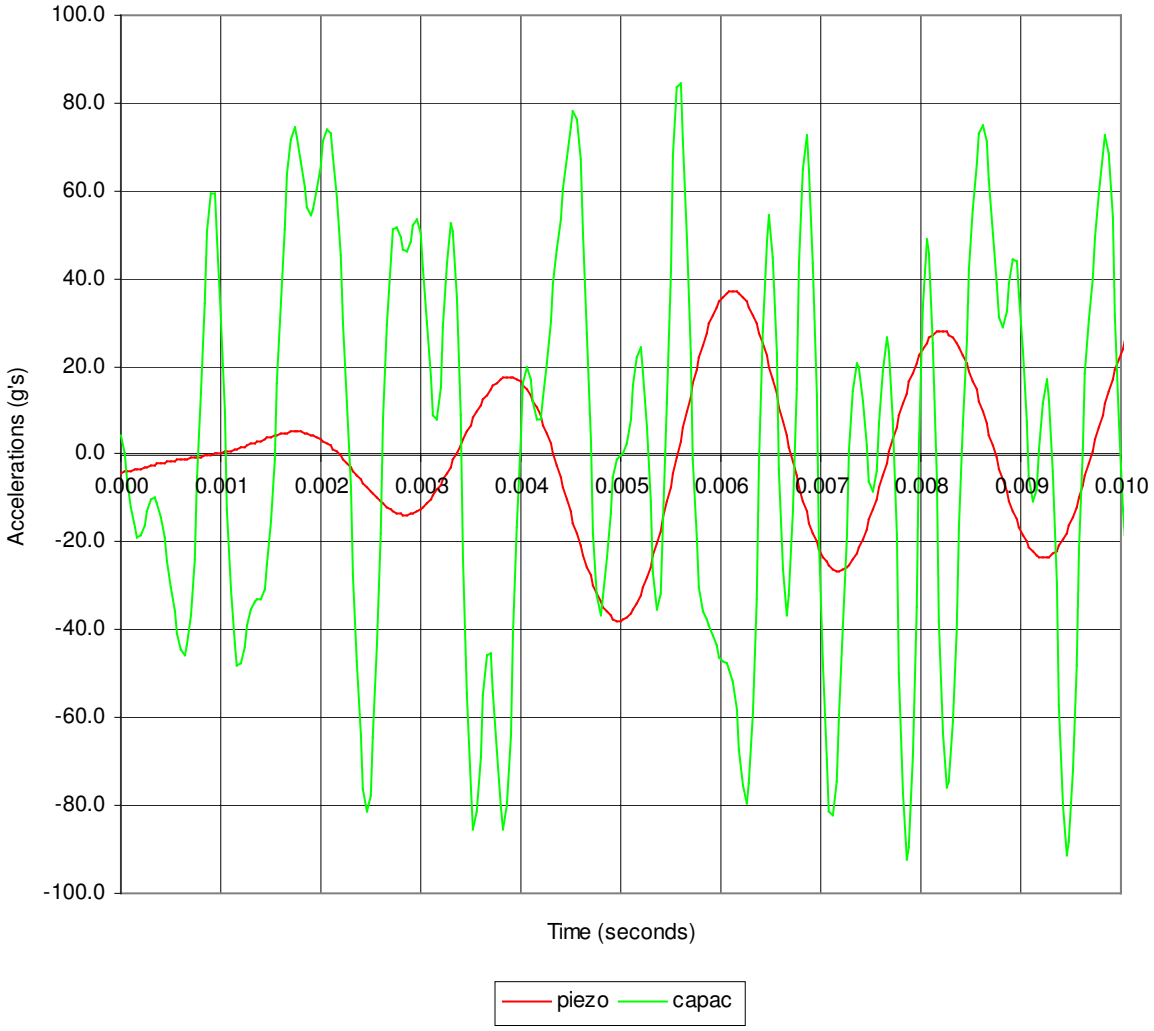

Figure B.4: Bracket Impact Accelerations - Test 2

Appendix B (Continued)

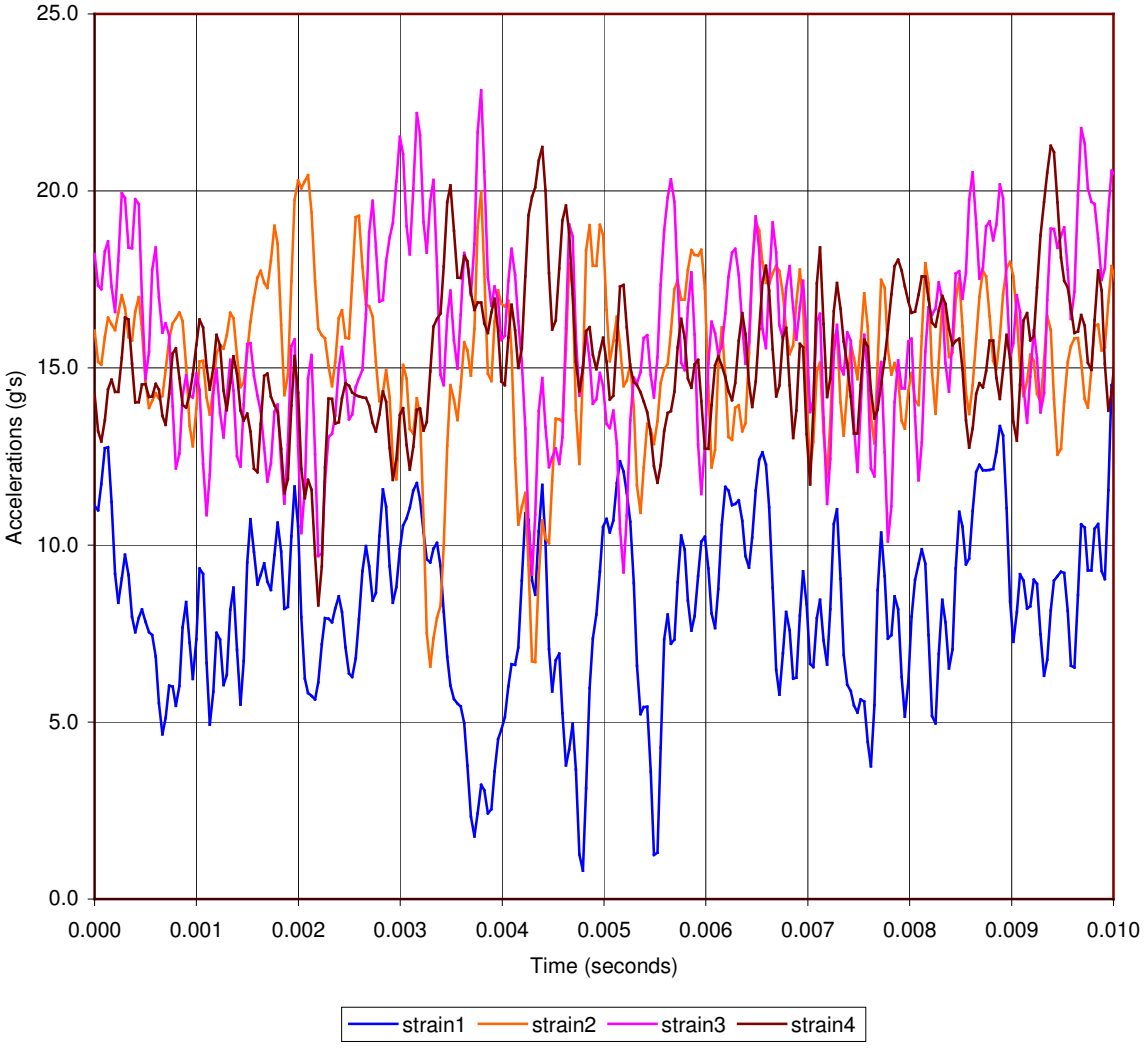

Figure B.5: Bracket Impact Strain Data - Test 2